Electronic Supplementary Information

Mercury^{II}-mediated base pairs in DNA: unexpected behavior in metal ion binding and duplex stability induced by 2'-deoxyuridine 5-substituents

Xiurong Guo[a,b], Sachin A. Ingale[b,c], Haozhe Yang[b,c], Yang He[a], and Frank Seela[b,c]*

[a]Precision Medicine Research Laboratory, West China Hospital, West China School of Medicine, Sichuan University, 610041 Chengdu, People's Republic of China,[b]Laboratory of Bioorganic Chemistry and Chemical Biology, Center for Nanotechnology, Heisenbergstrasse 11, 48149 Münster, Germany, and [c]Laboratorium für Organische und Bioorganische Chemie, Institut für Chemie neuer Materialien, Universität Osnabrück, Barbarastrasse 7, 49069 Osnabrück, Germany

Corresponding author: Prof. Dr. Frank Seela
Phone: +49 (0)251 53 406 500; Fax: +49 (0)251 53 406 857
E-mail: Frank.Seela@uni-osnabrueck.de
Homepage: www.seela.net

Table of Contents

Table S1 ^{13}C NMR data of 5-substituted 2'-deoxyuridine nucleosides[a,b]

	C2	C4	C5	C6	5-substitutents	C-1'	C-2'	C-3'	C-4'	C-5'
2[1]	149.9	161.6	112.1	146.5	193.4, 30.2	85.5	-[c]	70.2	87.9	61.0
17[d]	150.0	161.7	112.3	146.4	193.5, 30.6	86.6	-[c]	70.8	86.4	64.0
11	163.0	169.4	116.0	154.3	6.8, 5.8	-	-	-	-	-
12	164.4	150.8	113.4	135.7	7.4, 5.1	-	-	-	-	-
13a	149.9	163.3	115.6	134.2	8.0, 5.3, 5.2	84.9	36.0	74.7	81.2	64.2
13b	149.7	163.4	114.3	134.1	8.2, 5.2, 4.6	86.1	37.2	74.6	83.4	63.9
3[2]	149.8	163.3	115.1	134.1	7.7, 5.4, 5.3	83.8	-[c]	70.1	87.0	60.9
18	149.8	163.1	115.0	134.0	8.1, 4.9	83.8	39.0	70.3	85.2	63.6
16	149.5	161.8	104.5	140.3	145.8, 142.4, 134.3, 121.7, 117.7, 112.3,	85.2	37.2	74.1	81.9	63.7
9[3]	149.5	161.8	103.9	140.9	146.0,121.6, 117.9, 112.2	85.3	-[c]	70.5	87.8	61.3
19	149.4	161.9	103.7	140.6	145.9, 142.5, 134.3,121.6, 121.5,117.9,112.2	86.1	40.7	70.5	85.9	63.6
4[4]	149.5	161.6	97.5	144.5	83.6, 76.4	84.7	-[c]	70.9	87.5	61.8
7[d]	149.4	161.4	99.5	144.4	98.3, 93.0, 52.6, 18.5, 10.7	84.9	-[c]	69.8	87.6	60.7
14[1]	148.7	160.9	98.3	144.1	98.3, 93.3, 54.4, 17.8, 10.1	84.8	-[c]	69.9	85.3	63.1

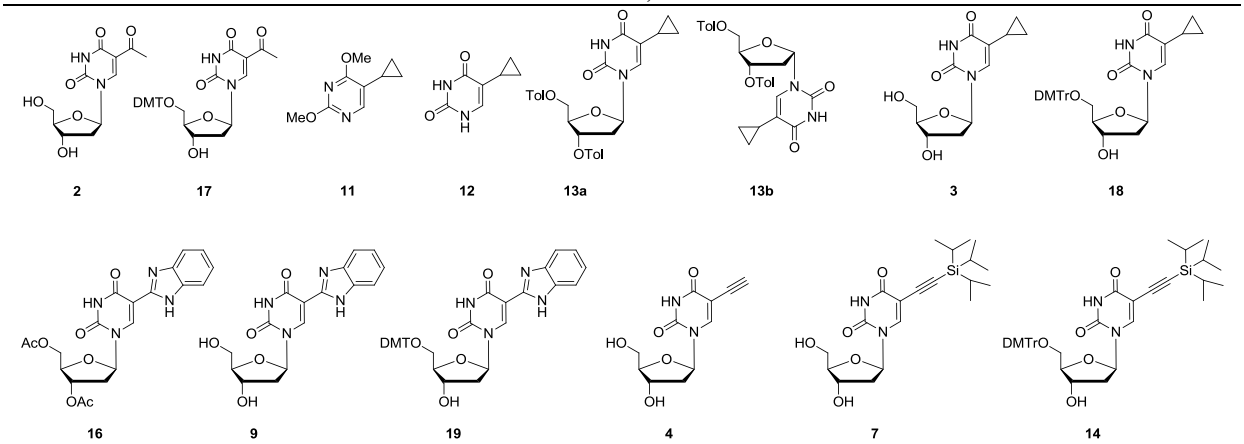

[a]Measured in DMSO-d_6 at 298 K. [b]Pyrimidine numbering. [c]Superimposed by DMSO. [d]Assigned by 2D spectra (HSQC and HMBC). All the other assignments were done by using ^{1}H-^{13}C gated-decoupled spectra and DEPT-135 spectra.

Table S2 Selected ^{1}H-^{13}C coupling constants (Hz) of 5-substituted 2'-deoxyuridine nucleosides[a,b]

^{1}H-^{13}C coupling constants	**11**	**13a**	**13b**	**18**	**16**	**19**
^{1}J(C6, H-C6)	178.2	178.3	177.8	177.3	183.0	184.5
^{3}J(C6, H-C1')	4.3	n.d	n.d.	4.8	3.5	4.3
^{3}J(C2, H-C6) or ^{3}J(C2, H-C1')	9.5	7.8	8.2	7.9	8.3	8.3
^{3}J(C4, H-C6)	9.4	10.0	10.0	10.0	9.2	9.4
^{1}J(C1', H-C1')	-	167.4	168.7	169.0	170.5	167.2
^{1}J(C3', H-C3')	-	161.4	154.0	147.2	159.2	150.0
^{1}J(C4', H-C4')	-	153.6	154.3	149.0	152.3	151.9
^{1}J(C5', H-C5')	-	152.6	149.4	142.4	147.9	141.7

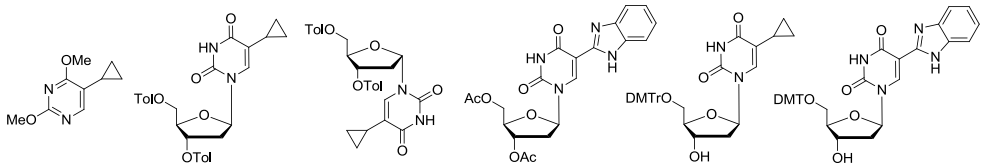

11 **13a** **13b** **16** **18** **19**

[a]Measured in DMSO-d_6 at 298 K. [b]Pyrimidine numbering. n.d.: not detected.

pK_a Determination by UV

Nucleosides (**2**, **3**, **4**, or **7**) were dissolved in 0.1 M sodium phosphate buffer, pH 4.5. An aqueous NaOH solution (4 M) and concentrated phosphorus acid were used to adjust the pH value of the buffer. At defined pH values, the UV absorbance of nucleosides was measured (Fig. S1).

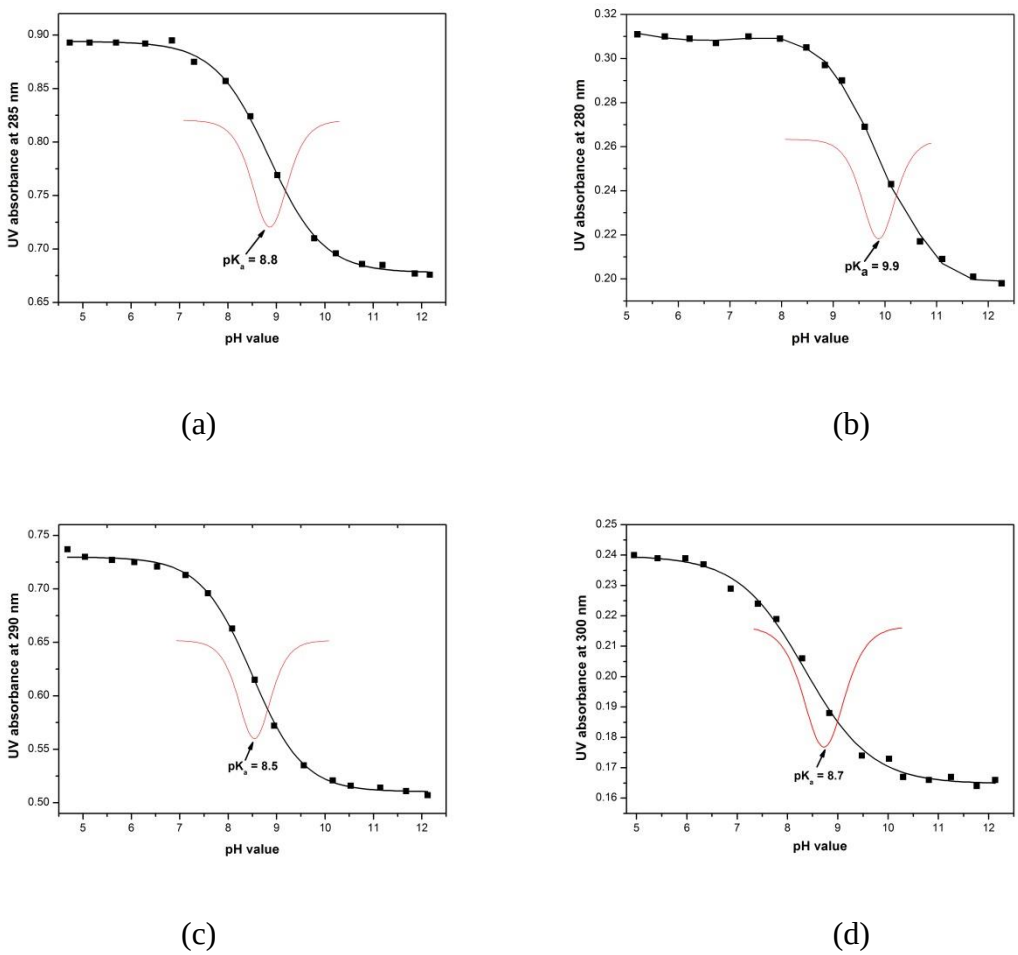

Fig. S1 UV absorbance *vs* pH. (a) Nucleoside **2** at 285 nm; (b) nucleoside **3** at 280 nm; (c) nucleoside **4** at 290 nm; (d) nucleoside **7** at 300 nm. All measurements were performed in 0.1 M sodium phosphate buffer.

Reversed-phase HPLC profiles of purified oligonucleotides determined at 260 nm.

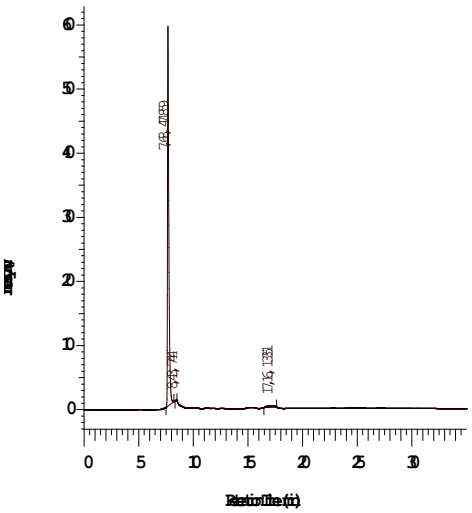

(a) 5’-d(TAG GTC **2**AT ACT) ODN **29**

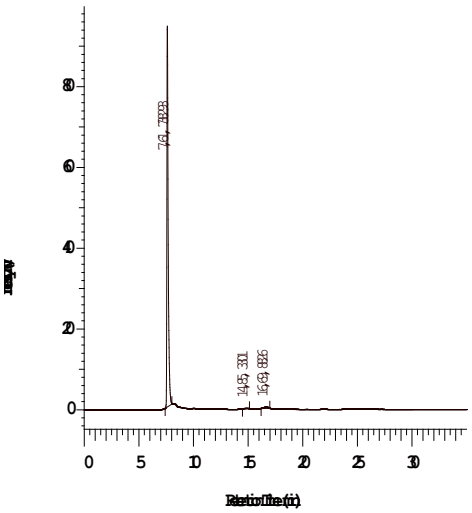

(b) 5’-d(AGT AT**2** GAC CTA) ODN **30**

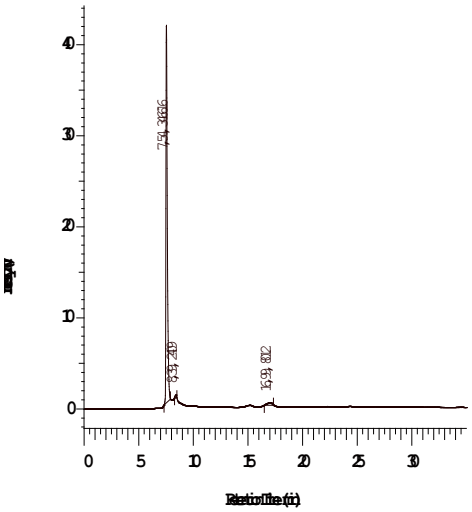

(c) 5’-d(TAG GTC **3**AT ACT) ODN **31**

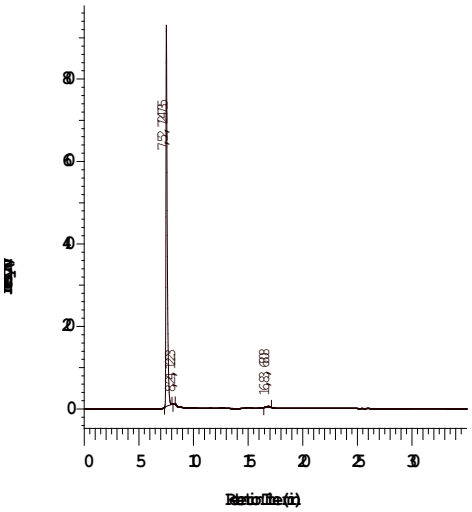

(d) 5’-d(AGT AT**3** GAC CTA) ODN **32**

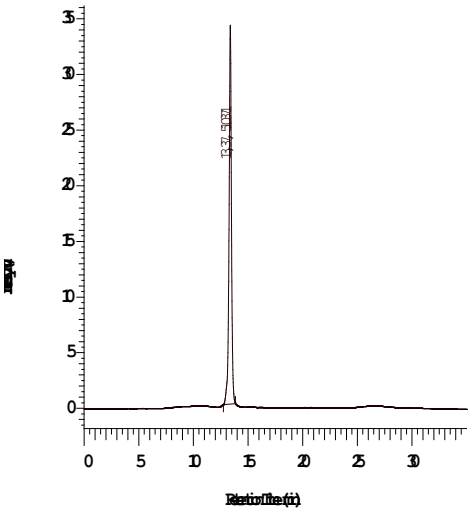

(e) 5’-d(TAG GTC **5**AT ACT) ODN **35**

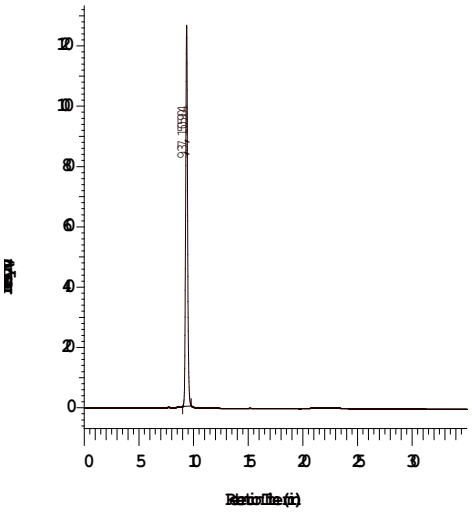

(f) 5’-d(AGT AT**5** GAC CTA) ODN **36**

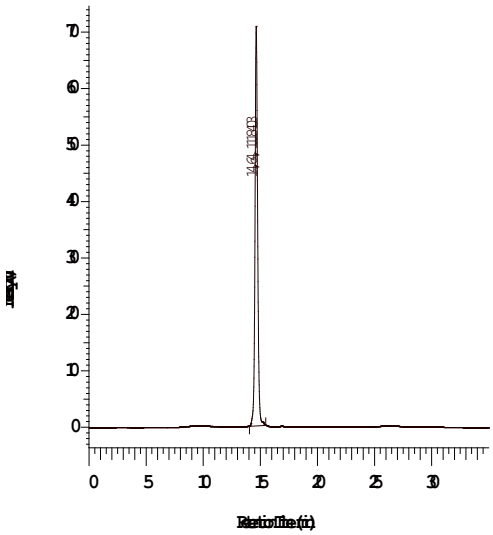

(g) 5’-d(TAG GTC **6**AT ACT) ODN **37**

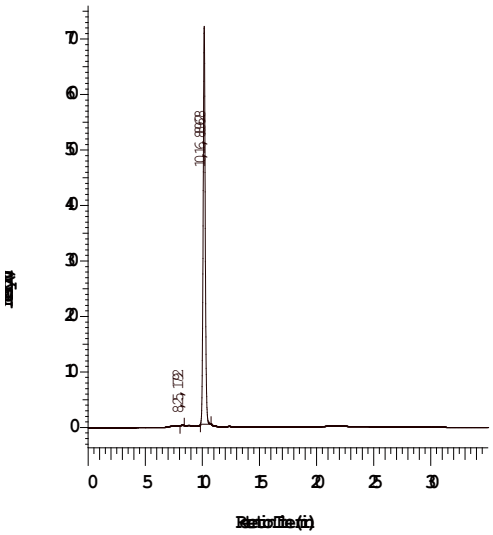

(h) 5’-d(AGT AT**6** GAC CTA) ODN **38**

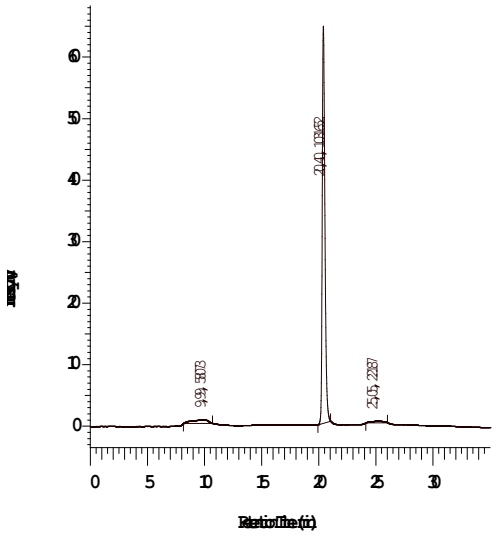

(i) 5’-d(TAG GTC **7**AT ACT) ODN **39**

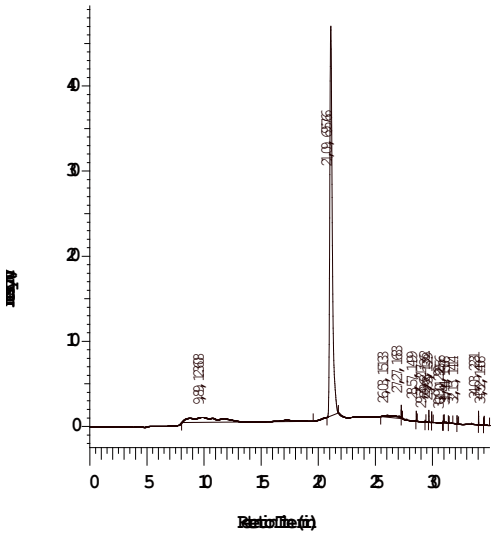

(j) 5’-d(AGT AT**7** GAC CTA) ODN **40**

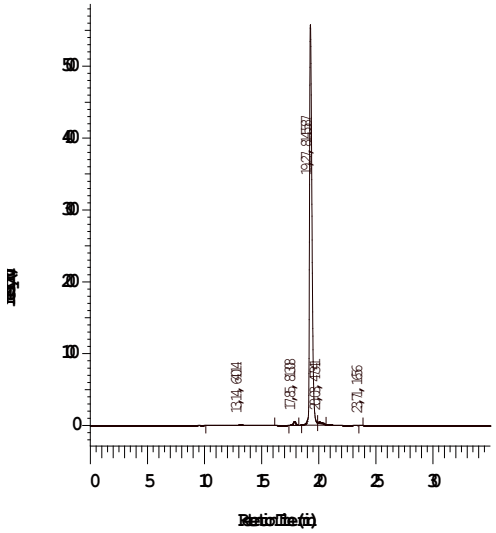

(k) 5’-d(TAG GTC **9**AT ACT) ODN **43**

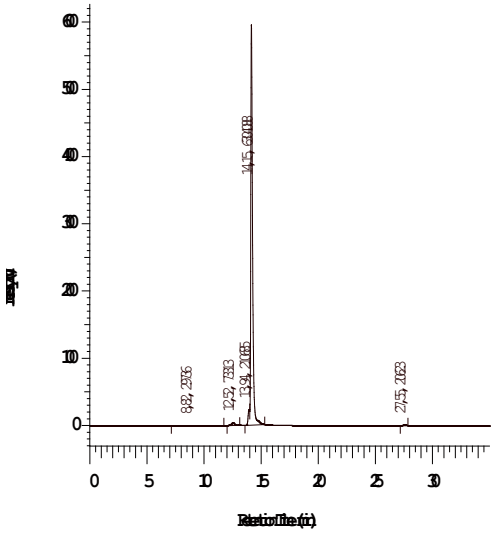

(l) 5’-d(AGT AT**9**GAC CTA) ODN **44**

Fig. S2 HPLC purity profiles of oligonucleotides. (a) ODN **29**; (b) ODN **30**; (c) ODN **31**; (d) ODN **32**; (e) ODN **35**; (f) ODN **36**; (g) ODN **37**; (h) ODN **38**; (i) ODN **39**; (j) ODN **40**; (k) ODN **43**; (l) ODN **44**. For elution the following solvent system was used: 0.1 M $(Et_3NH)OAc$: MeCN (95:5) (pH 7.0) (A) and MeCN (B). Gradient: 0-20 min 0-20% B in A, 20-25 min 20% B in A, 25-30 min 20-0% B in A, flow rate 0.8 mL min^{-1}.

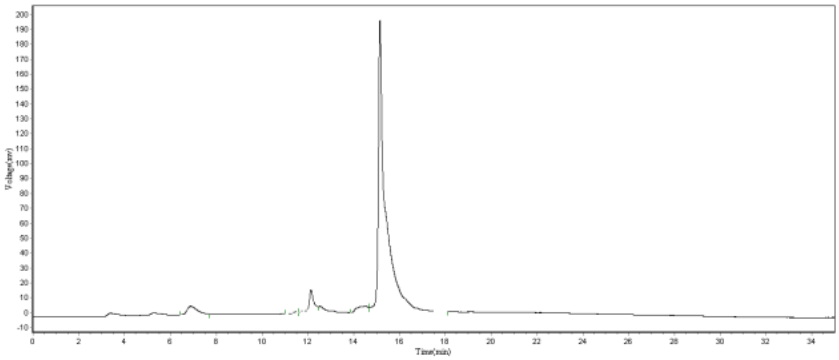

(a) 5’-d(TAG GTC **8**AT ACT) ODN **41**

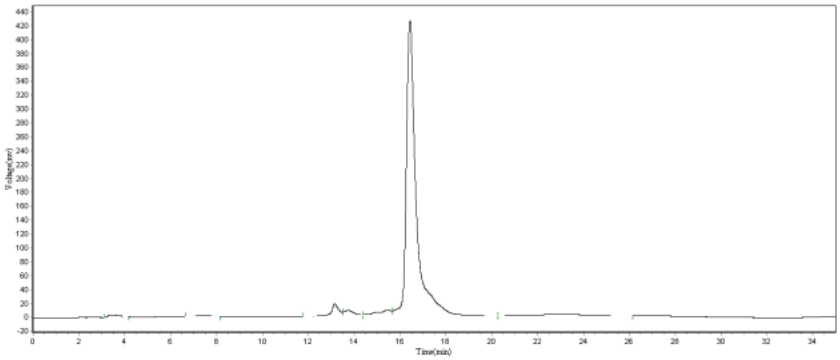

(b) 5’-d(AGT AT**8** GAC CTA) ODN **42**

Fig. S3 HPLC profiles of phenyltriazolyl modified oligonucleotides (crude mixture): (a) ODN **41**; (b) ODN **42**. For elution the following solvent system was used: 0.1 M $(Et_3NH)OAc$: MeCN (95:5) (pH 7.0) (A) and MeCN (B). Gradient: 0-20 min 0-20% B in A, 20-25 min 20% B in A, 25-30 min 20-0% B in A, flow rate 0.8 mL min^{-1}.

Melting profiles of duplexes

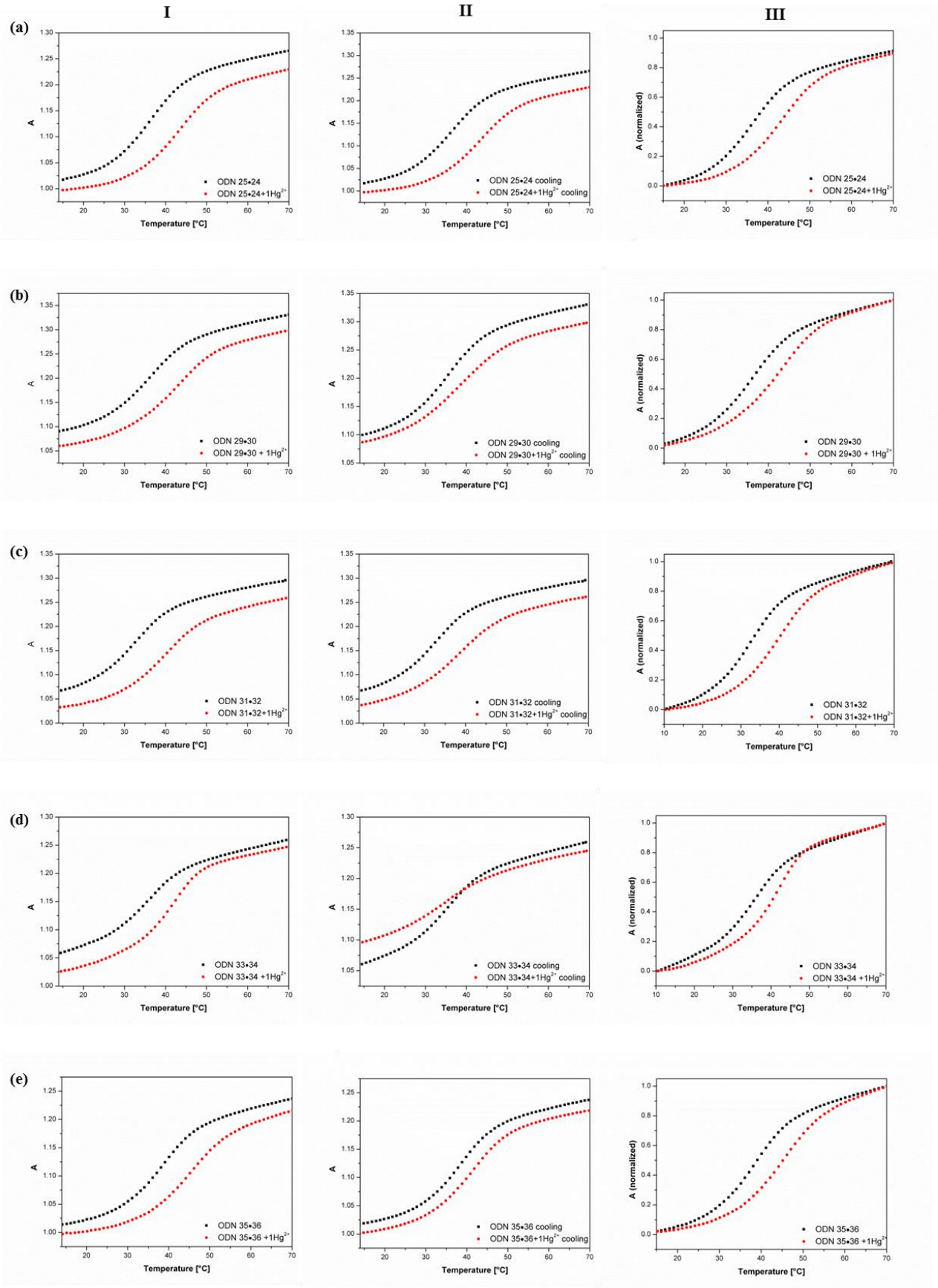

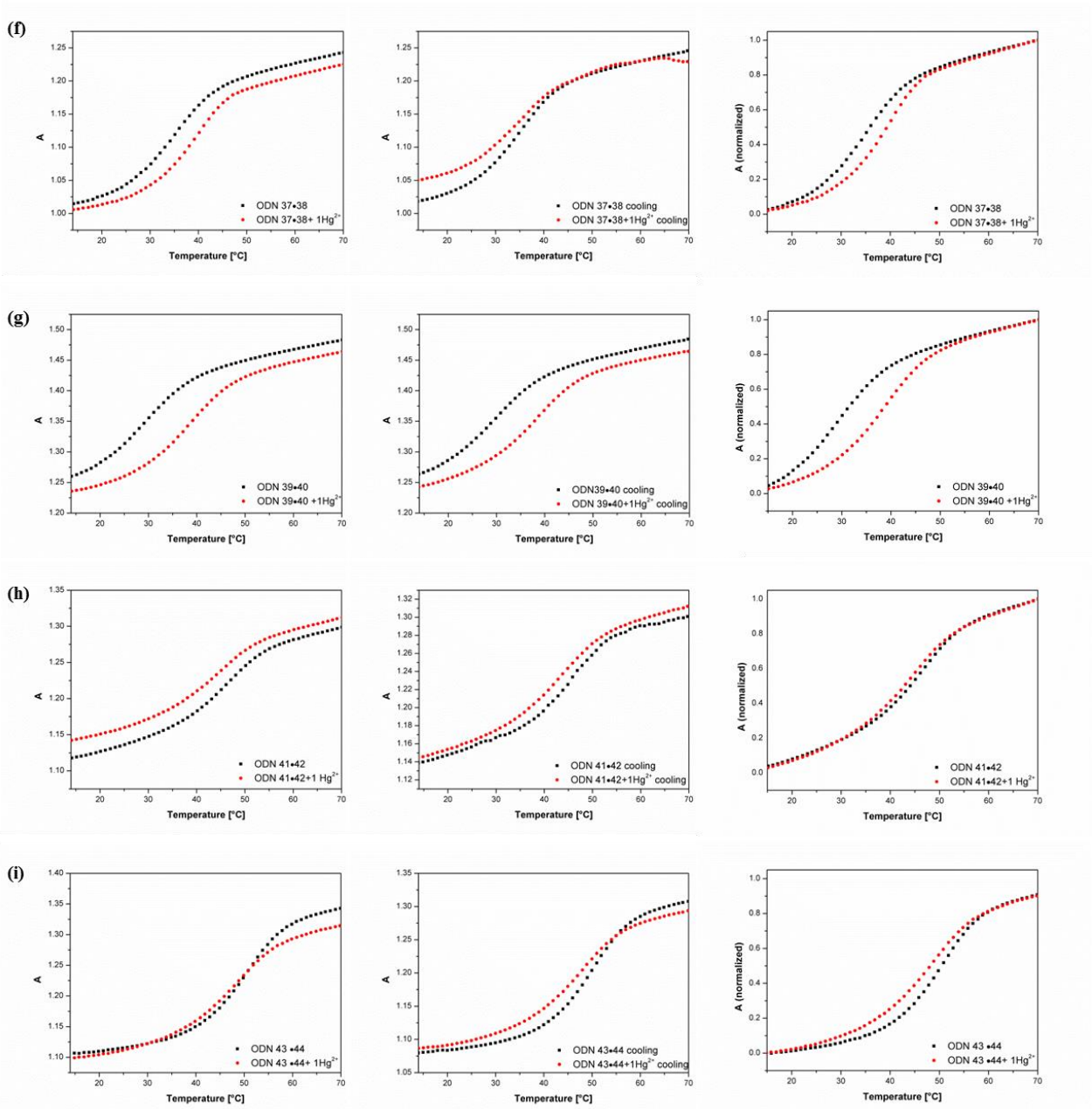

Fig. S4 The original and normalized melting curves of duplexes obtained from heating and cooling experiments with a single-strand concentration of 5 μM + 5 μM in 10 mM Mops, 100 mM $NaNO_3$ (pH 7.0) at 260 nm, absence and in presence of 1 equiv. of Hg^{2+}. Figures in column I: original melting curves (heating). Figures in column II: original melting curves (cooling). Figures in column III: normalized melting curves (heating). Relative absorbance A (normalized) = $(A-A_{min})/(A_{max}-A_{min})$ at 260 nm. : a) ODN **24•25**; b) ODN **29•30**; c) ODN **31•32**; d) ODN **33•34**; e) ODN **35•36**; f) ODN **37•38**; g) ODN **39•40**; h) ODN **41•42**; i) ODN **43•44**.

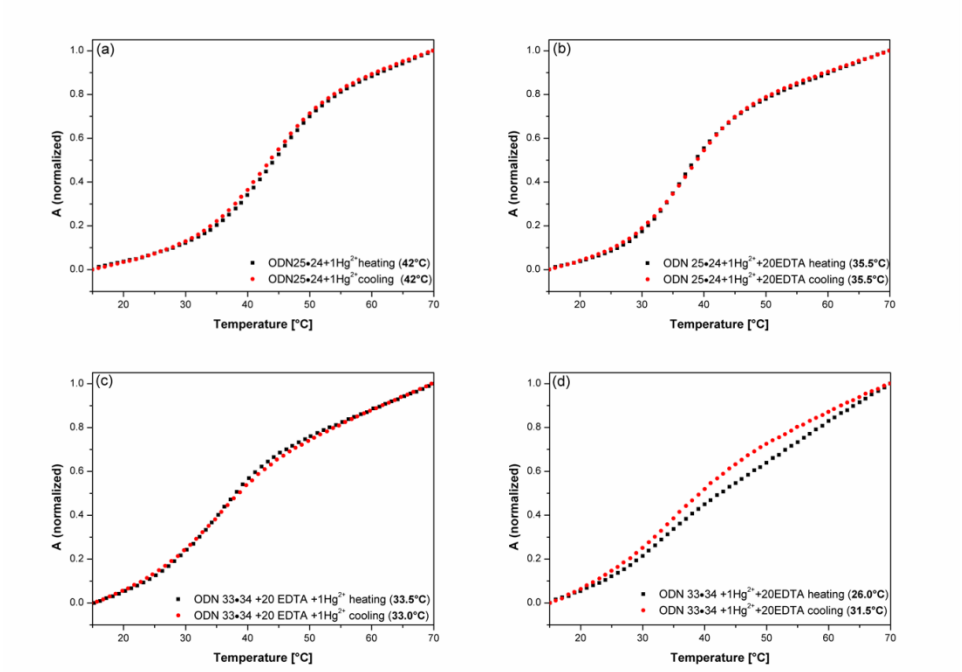

Fig. S5 The melting curves of duplexes obtained from heating and cooling experiments with a single-strand concentration of 5 μM + 5 μM in 10 mM Mops, 100 mM $NaNO_3$ (pH 7.0) at 260 nm, in presence of 1 equiv. of Hg^{2+}. Relative absorbance A(normalized) = $(A-A_{min})/(A_{max}-A_{min})$ at 260 nm: a) ODN **25•24** + $1Hg^{2+}$; b) ODN **25•24** + $1Hg^{2+}$ + 20 equiv. EDTA; c) ODN **33•34**+1 Hg^{2+}; d) ODN **33•34** + $1Hg^{2+}$ + 20 equiv. EDTA.

Stoichiometric titrations of oligonucleotides

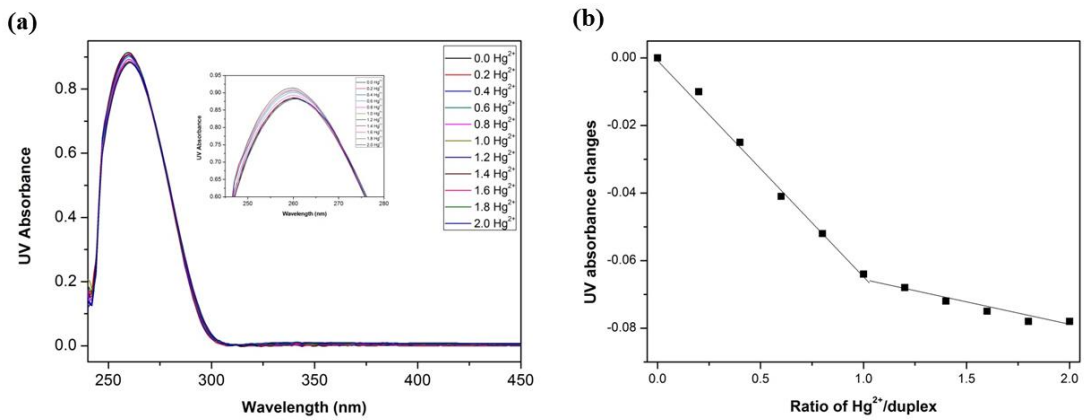

Fig. S6 (a) UV spectrophotometric titration of 5 μM ODN **25•24** with increasing concentration of Hg^{2+} ions (0–2.0 equiv.) in buffer (10 mM Mops, 100 mM $NaNO_3$, pH 7.0). (b) Graph of ratio of equivalents of Hg^{2+}/duplex *vs* changes in absorbance at 260 nm from (a).

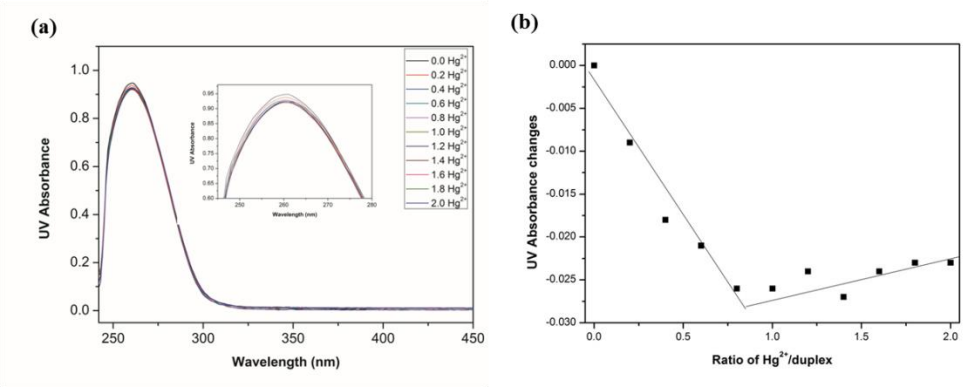

Fig. S7 (a) UV spectrophotometric titration of 5 μM ODN **29•30** with increasing concentration of Hg^{2+} ions (0–2.0 equiv.) in buffer (10 mM Mops, 100 mM $NaNO_3$, pH 7.0). (b) Graph of ratio of equivalents of Hg^{2+}/duplex *vs* changes in absorbance at 260 nm from (a).

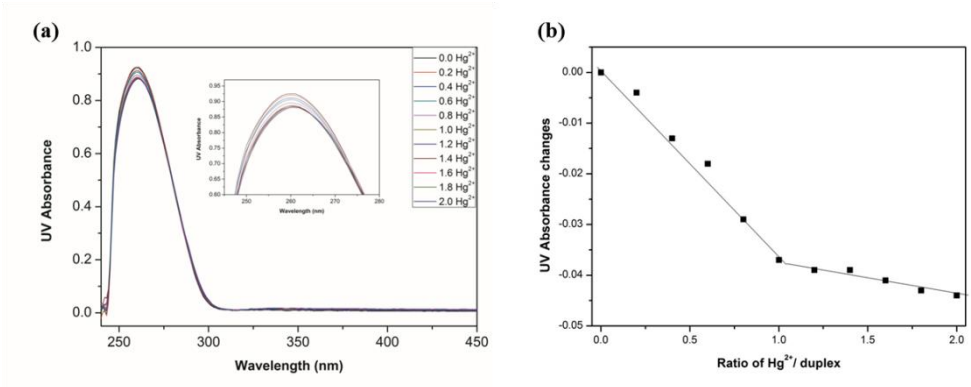

Fig. S8 (a) UV spectrophotometric titration of 5 μM ODN **31•32** with increasing concentration of Hg^{2+} ions (0–2.0 equiv.) in buffer (10 mM Mops, 100 mM $NaNO_3$, pH 7.0). (b) Graph of ratio of equivalents of Hg^{2+}/duplex *vs* changes in absorbance at 260 nm from (a).

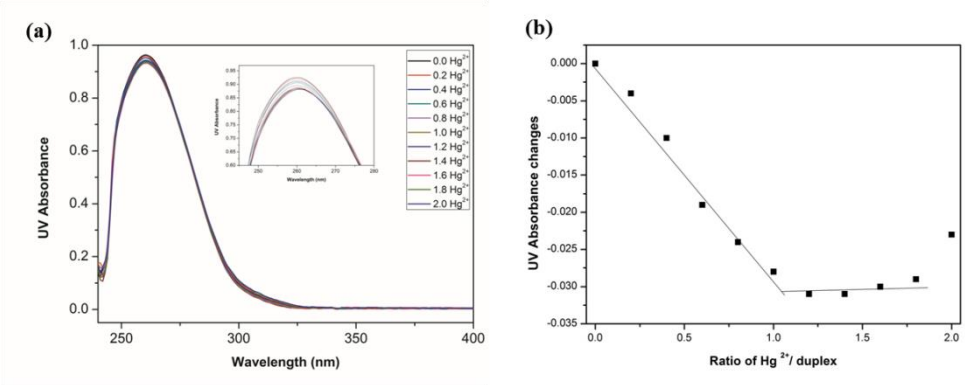

Fig. S9 (a) UV spectrophotometric titration of 5 μM ODN **33•34** with increasing concentration of Hg^{2+} ions (0–2.0 equiv.) in buffer (10 mM Mops, 100 mM $NaNO_3$, pH 7.0). (b) Graph of ratio of equivalents of Hg^{2+}/duplex *vs* changes in absorbance at 260 nm from (a).

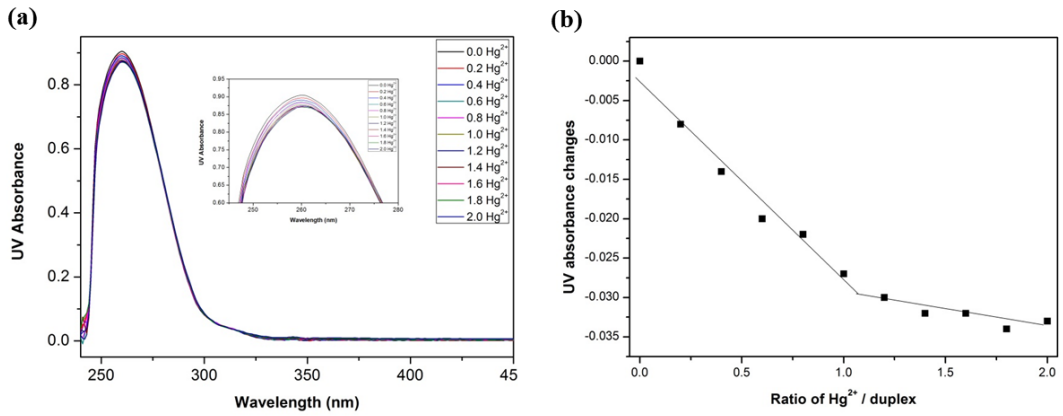

Fig. S10 (a) UV spectrophotometric titration of 5 μM ODN **35•36** with increasing concentration of Hg^{2+} ions (0–2.0 equiv) in buffer (10 mM Mops, 100 mM $NaNO_3$, pH 7.0). (b) Graph of ratio of equivalents of Hg^{2+}/duplex *vs* changes in absorbance at 260 nm from (a).

References

(1) S. A. Ingale, H. Mei, P. Leonard and F. Seela, *J. Org. Chem.*, 2013, **78**, 11271-11282.

(2) I. Basnak, A. Balkan, P. L. Coe and R. T. Walker, *Nucleos. Nucleot.*, 1994, **13**, 177-196.

(3) J. Krim, C. Grünewald, M. Taourirte and J. W. Engels, *Bioorg. Med. Chem.*, 2012, **20**, 480-486.

(4) V. Borsenberger, M. Kukwikila and S. Howorka, *Org. Biomol. Chem.*, 2009, **7**, 3826-3835.

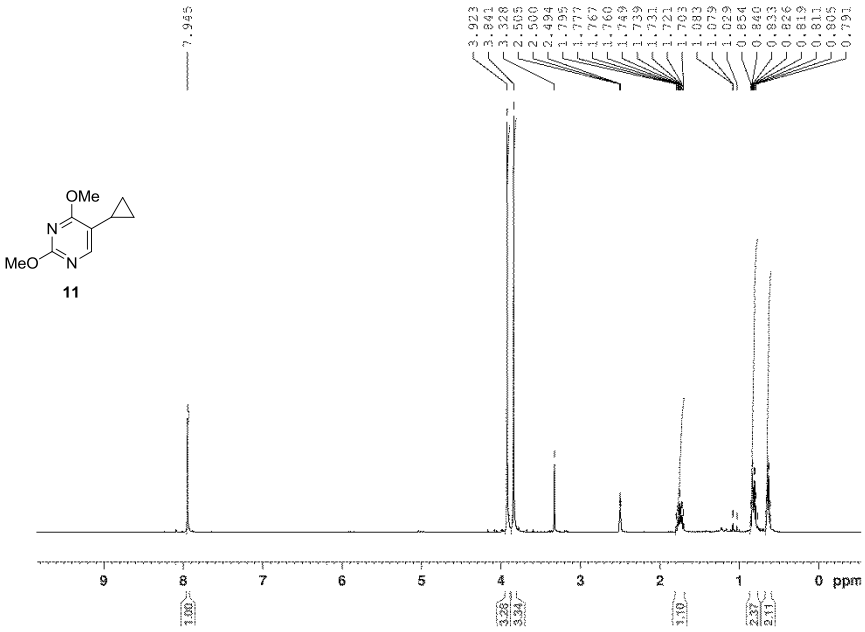

Fig. S11 ^{1}H NMR spectrum of compound **11**.

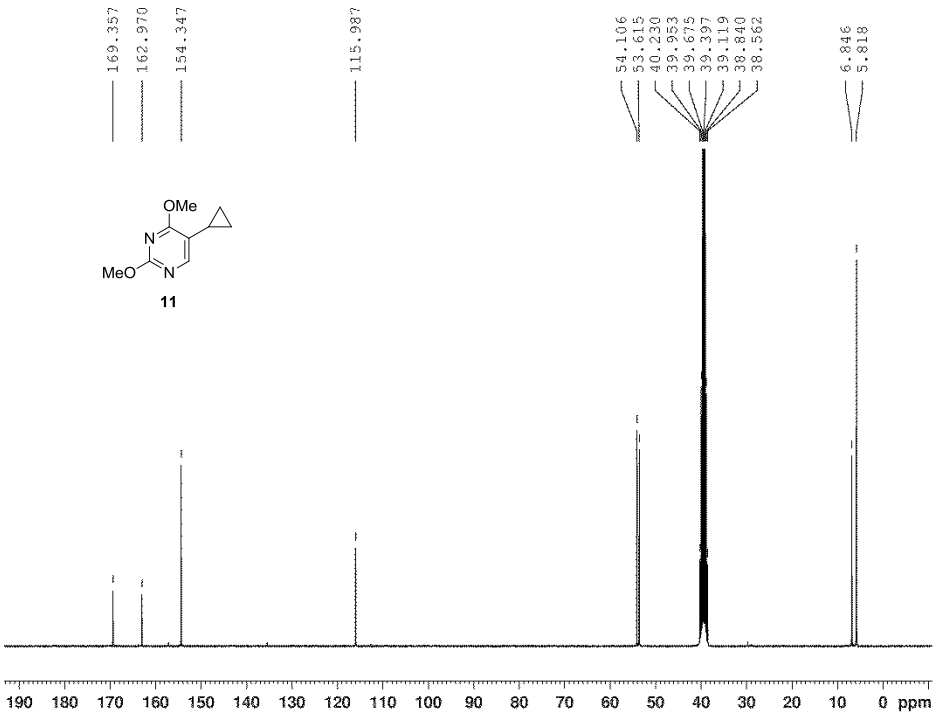

Fig. S12 ^{13}C NMR spectrum of compound **11**.

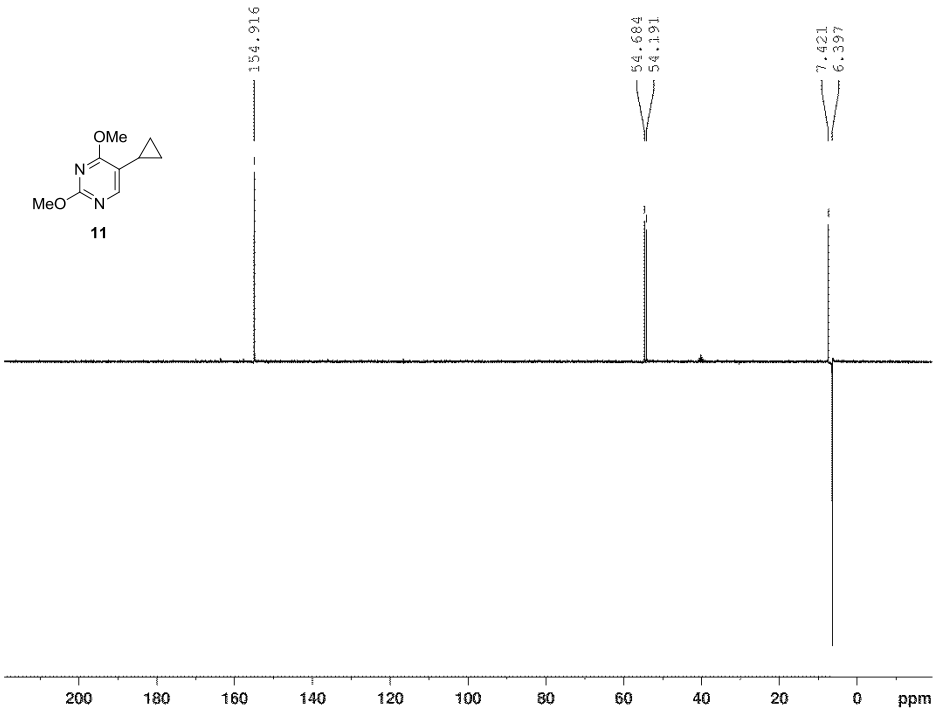

Fig. S13 DEPT-135 spectrum of compound **11**.

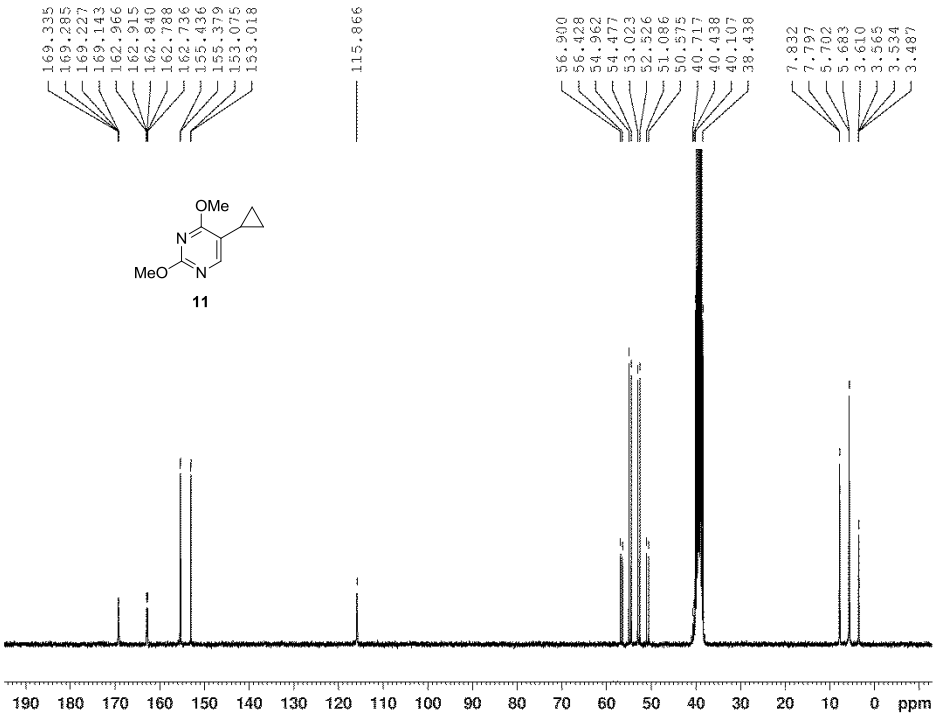

Fig. S14 ^{1}H-^{13}C gated-decoupled spectrum of compound **11**.

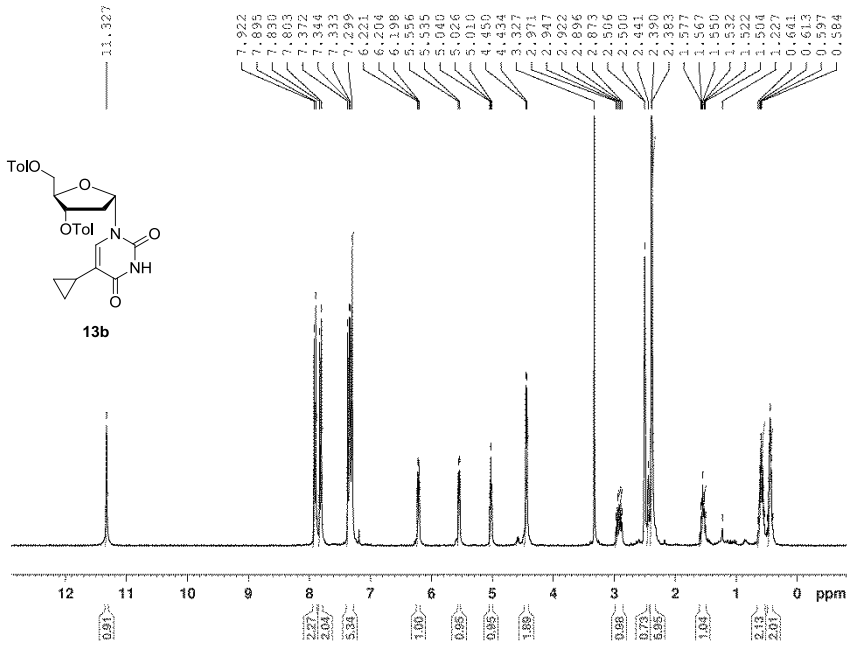

Fig. S15 ^{1}H NMR spectrum of compound **13b**.

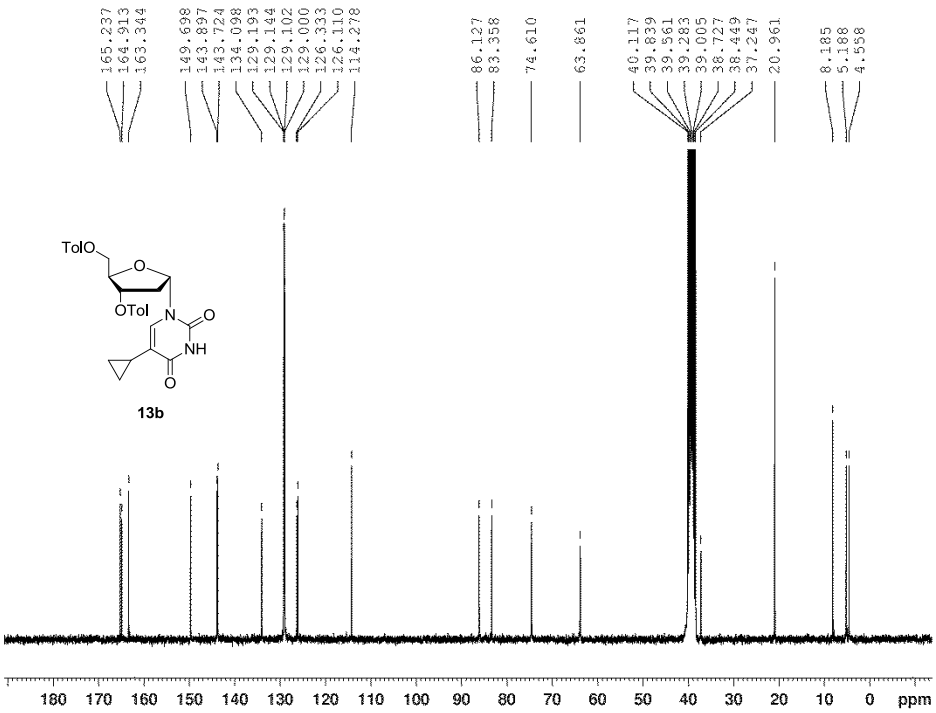

Fig. S16 ^{13}C NMR spectrum of compound **13b**.

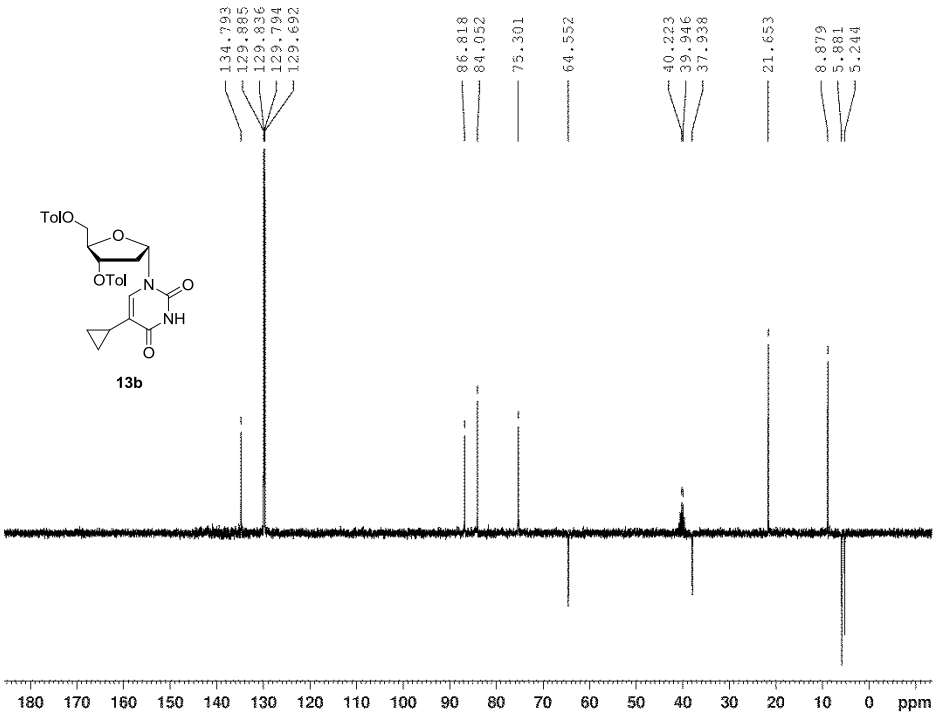

Fig. S17 DEPT-135 spectrum of compound **13b**.

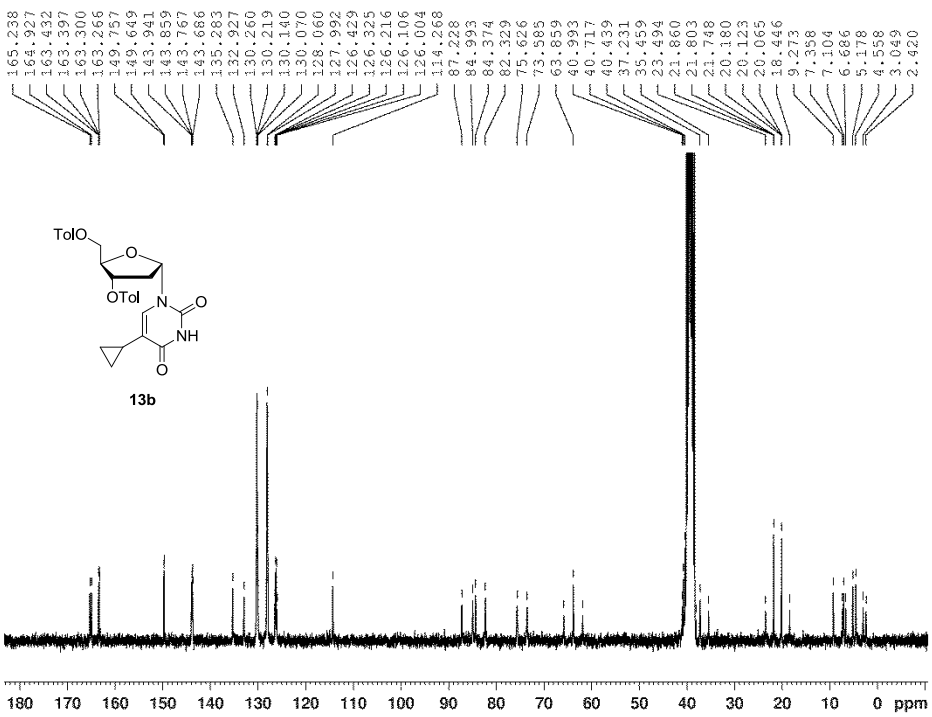

Fig. S18 ^{1}H-^{13}C gated-decoupled spectrum of compound **13b**.

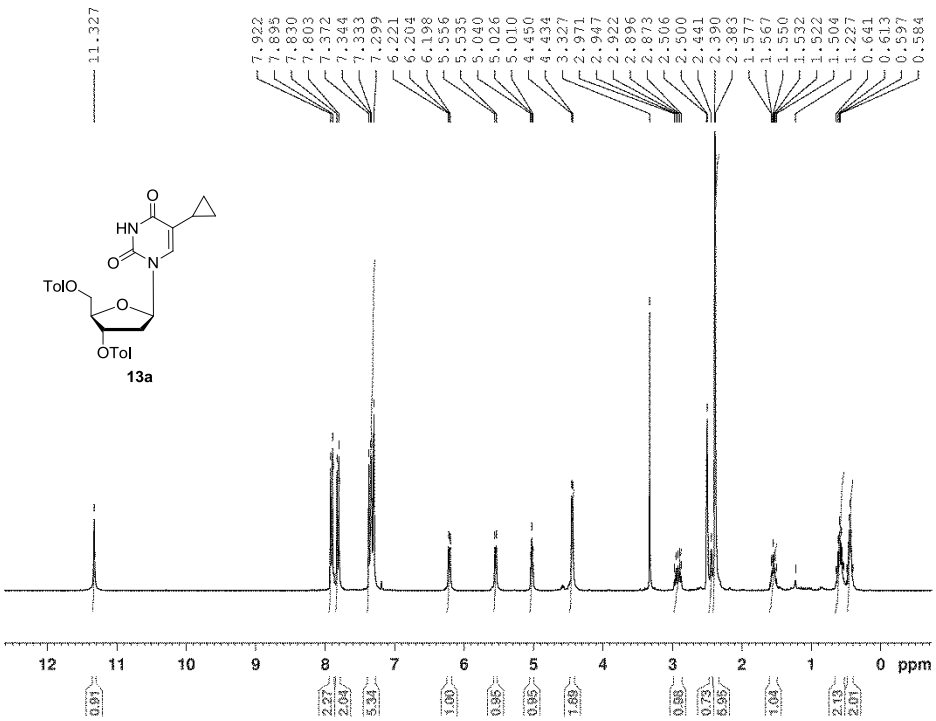

Fig. S19 ^{1}H NMR spectrum of compound **13a**

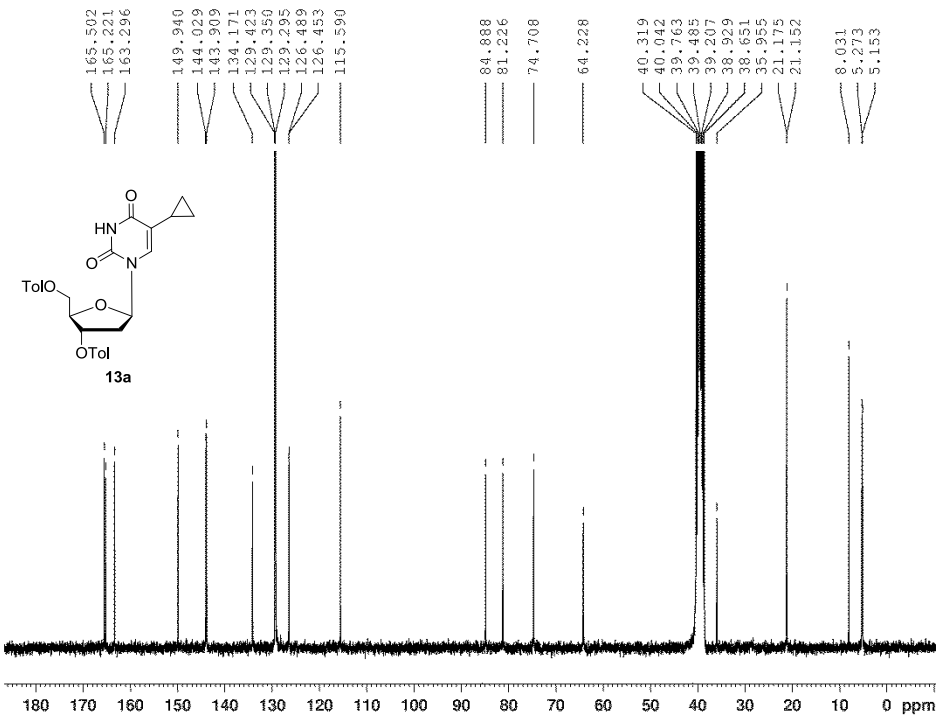

Fig. S20 ^{13}C NMR spectrum of compound **13a**.

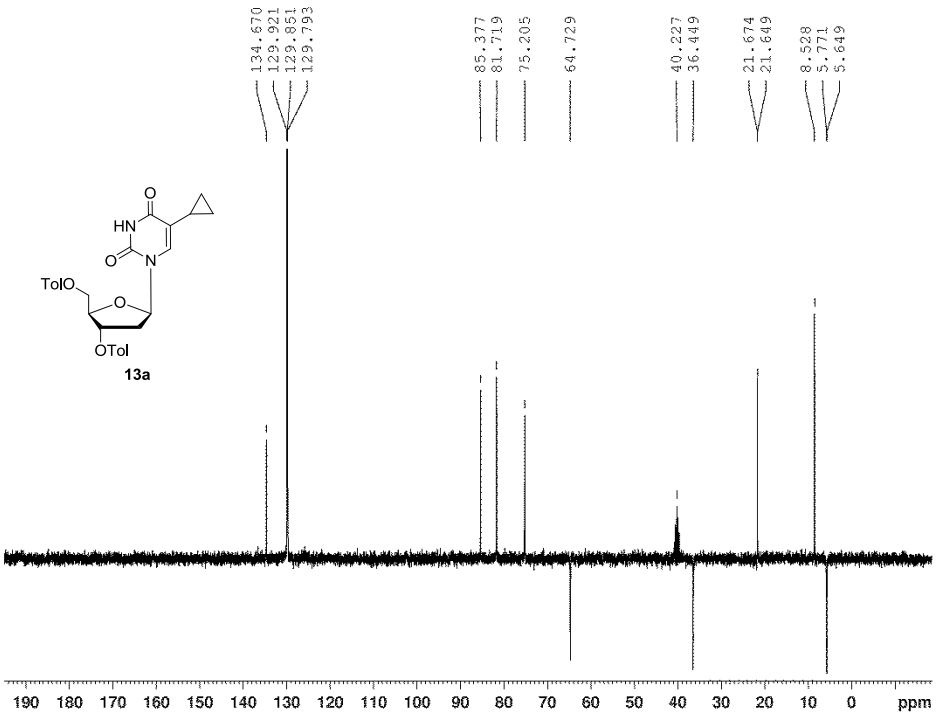

Fig. S21 DEPT-135 spectrum of compound **13a**

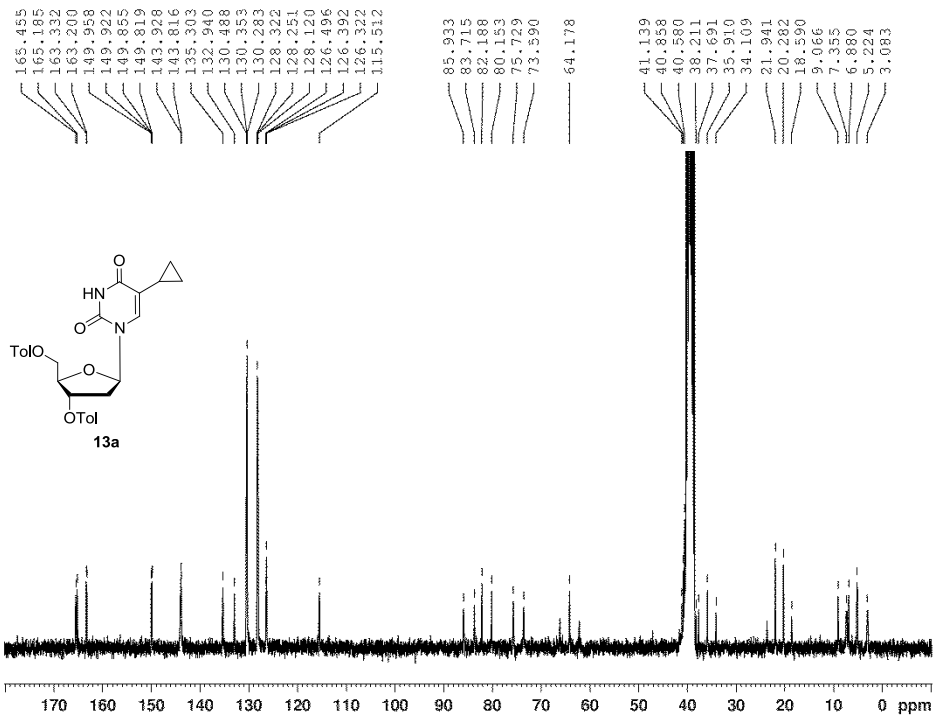

Fig. S22 ^{1}H-^{13}C gated-decoupled spectrum of compound **13a**.

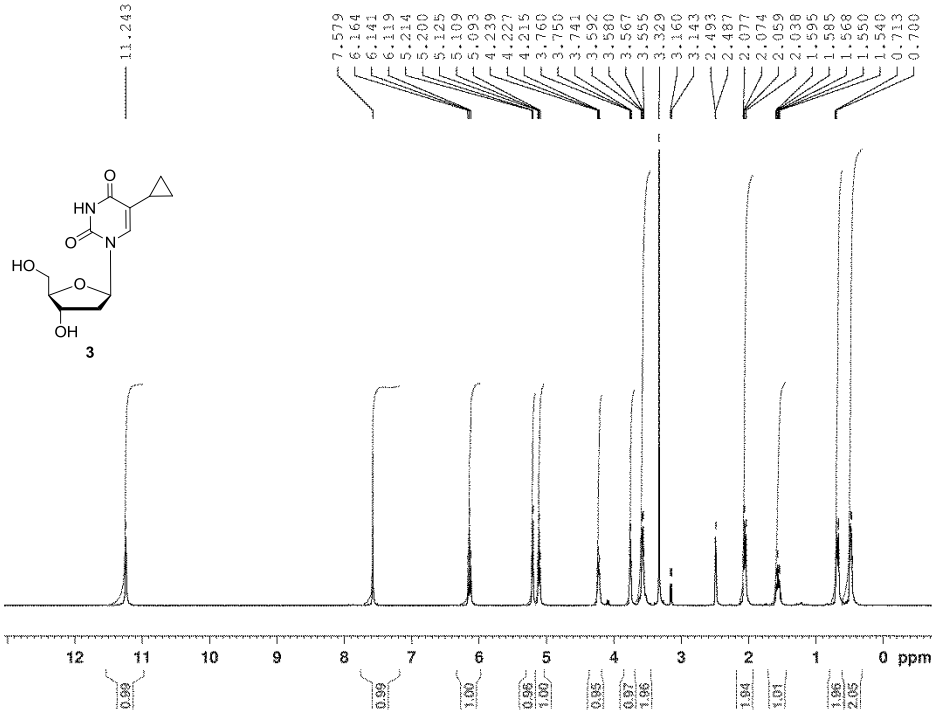

Fig. S23 ^{1}H NMR spectrum of compound **3**

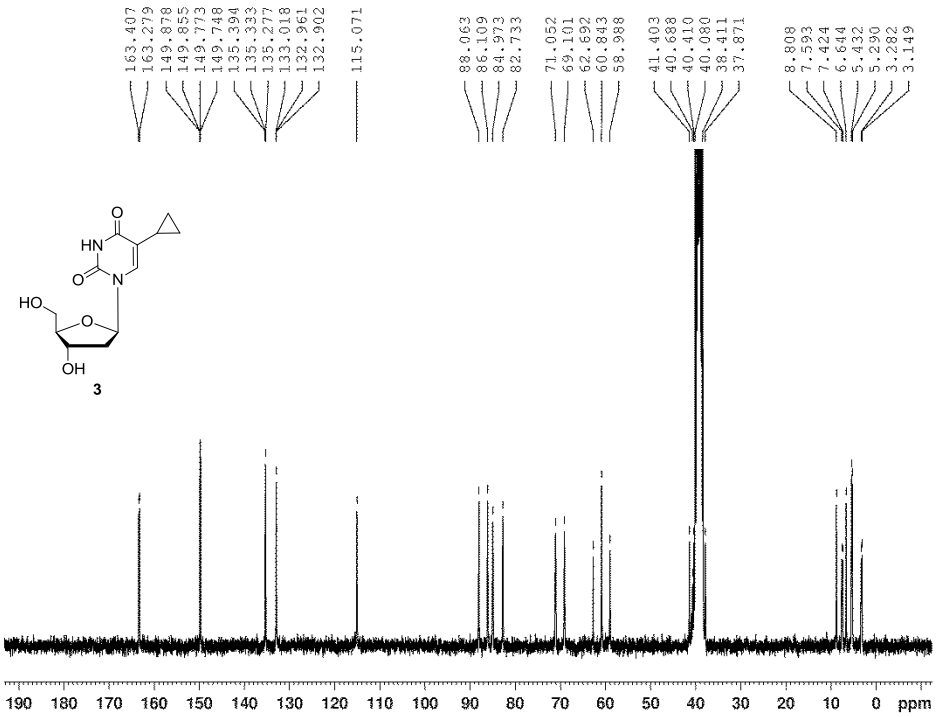

Fig. S24 ^{13}C NMR spectrum of compound **3**.

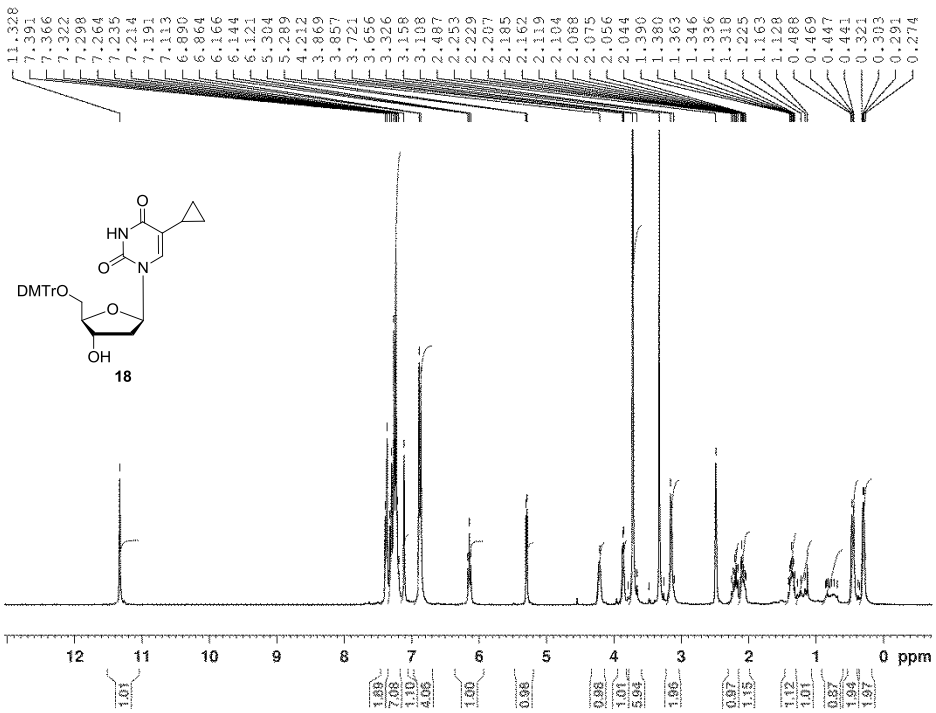

Fig. S25 ^{1}H NMR spectrum of compound **18**.

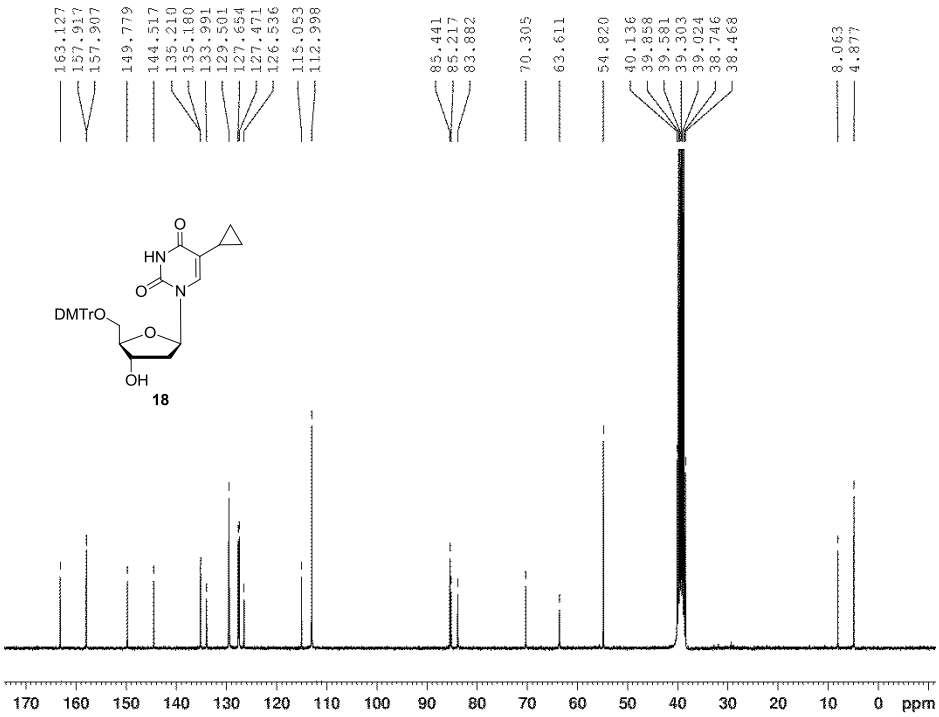

Fig. S26 ^{13}C NMR spectrum of compound **18**.

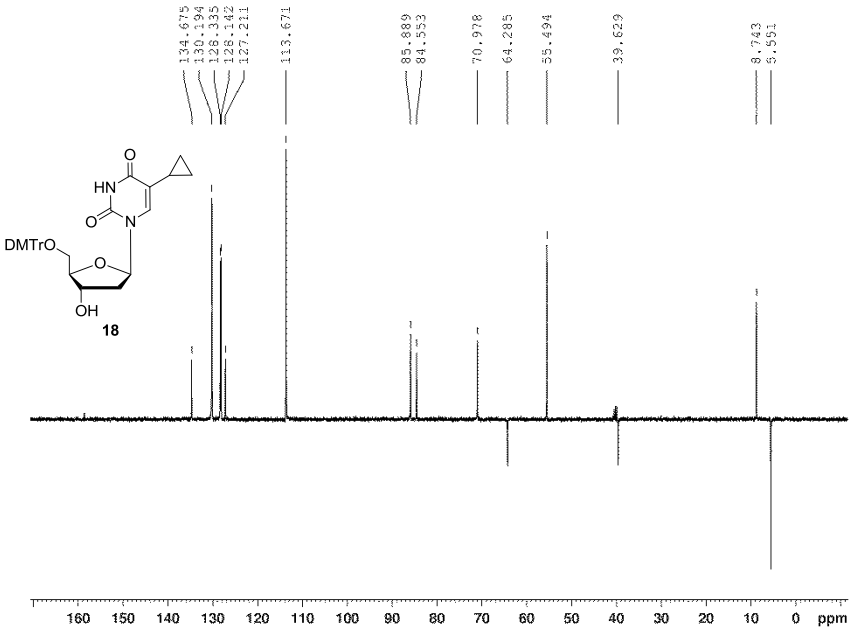

Fig. S27 DEPT-135 spectrum of compound **18**.

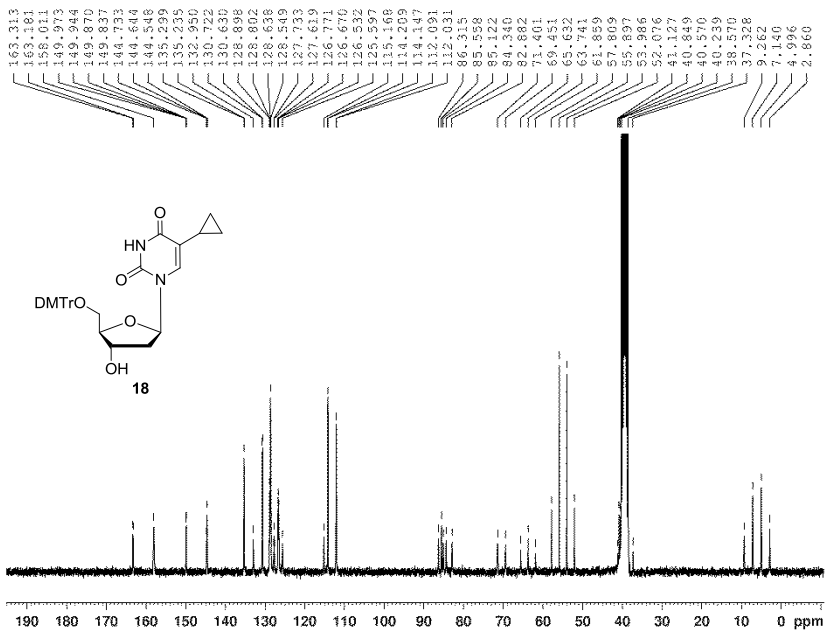

Fig. S28 ^{1}H-^{13}C gated-decoupled spectrum of compound **18**.

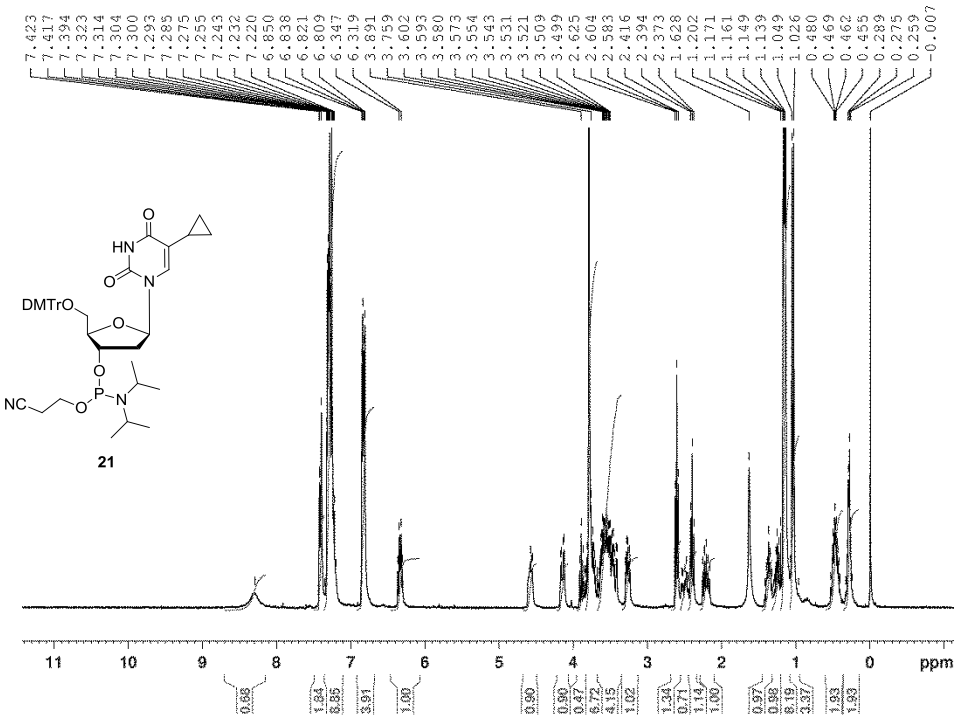

Fig. S29 ^{1}H NMR spectrum of compound **21**.

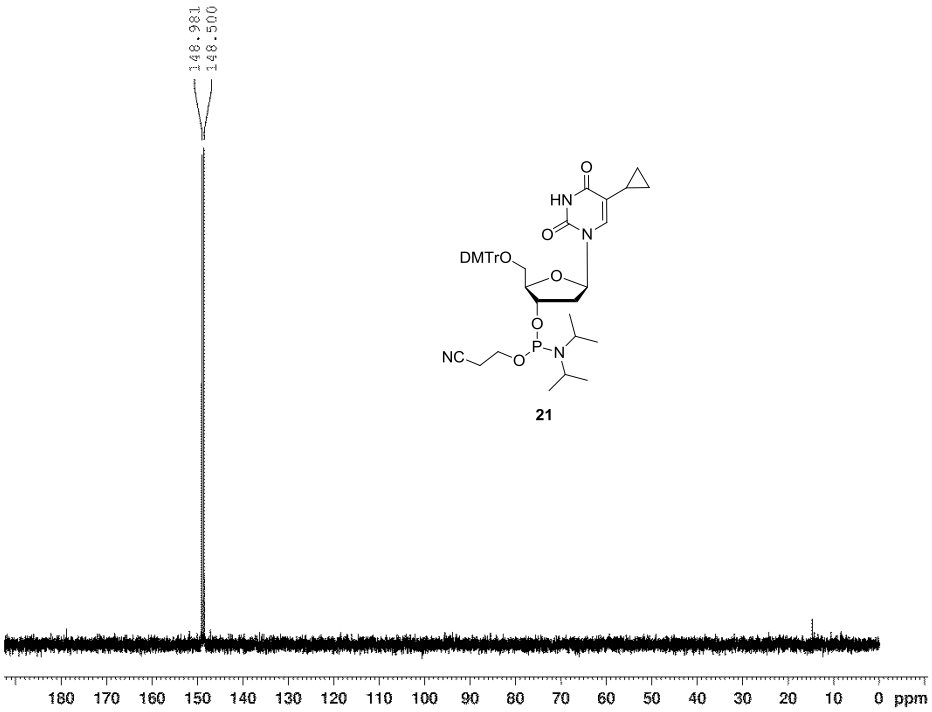

Fig. S30 ^{31}P NMR spectrum of compound **21**.

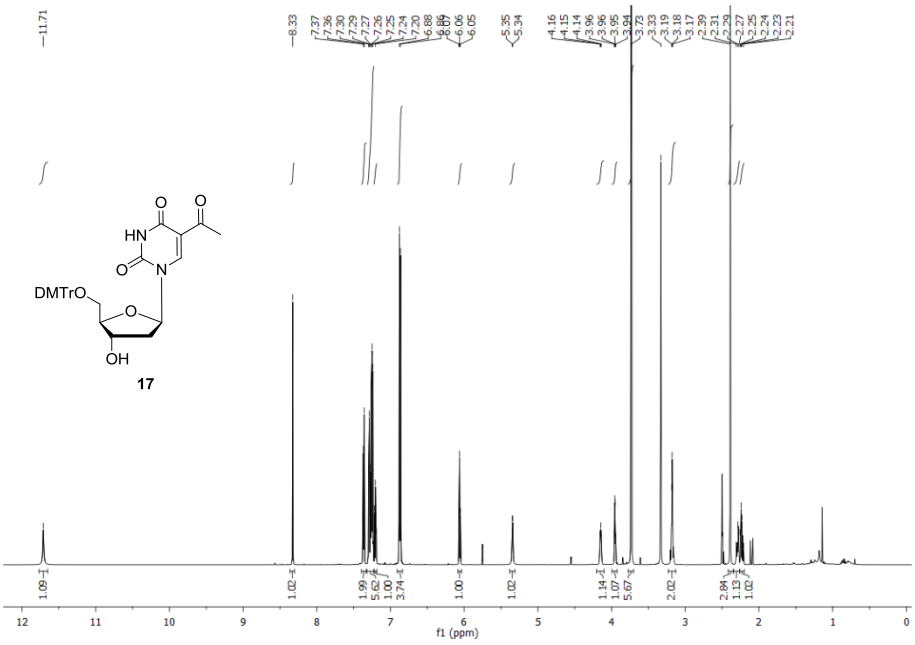

Fig. S31 ^{1}H NMR spectrum of compound **17**.

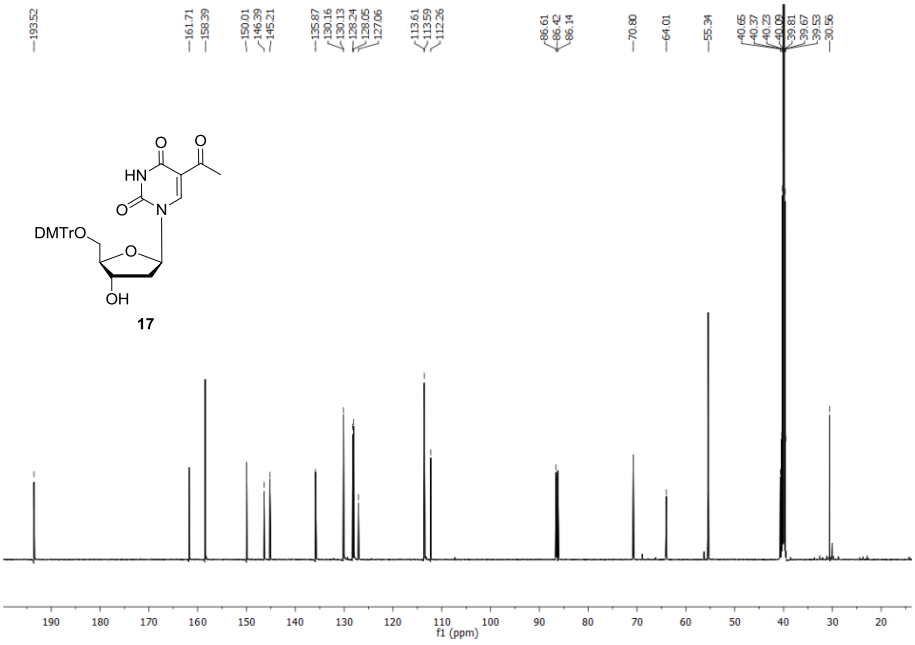

Fig. S32 ^{13}C NMR spectrum of compound **17**.

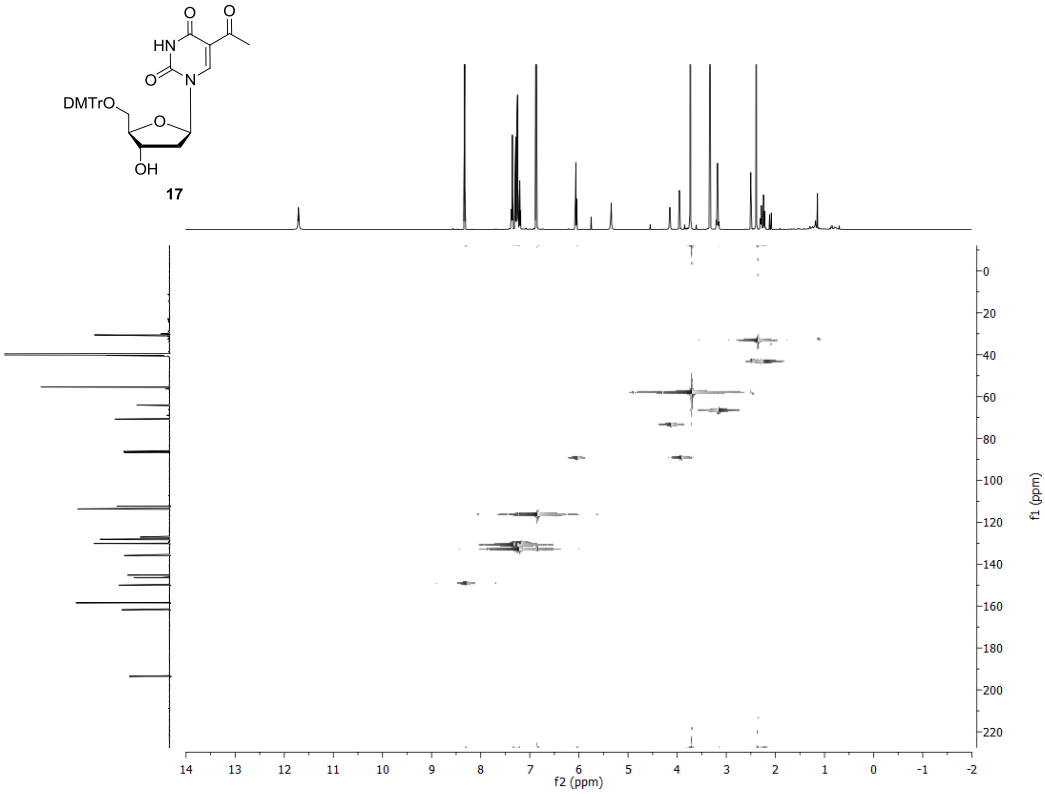

Fig. S33 HSQC spectrum of compound **17**.

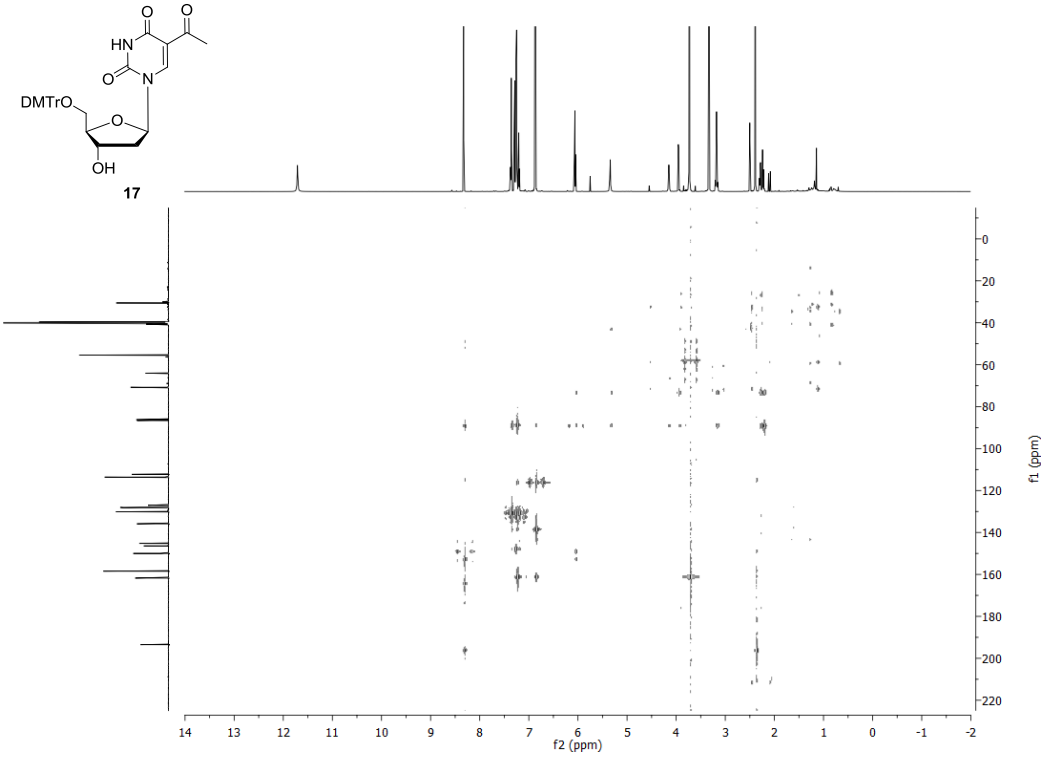

Fig. S34 HMBC spectrum of compound **17**.

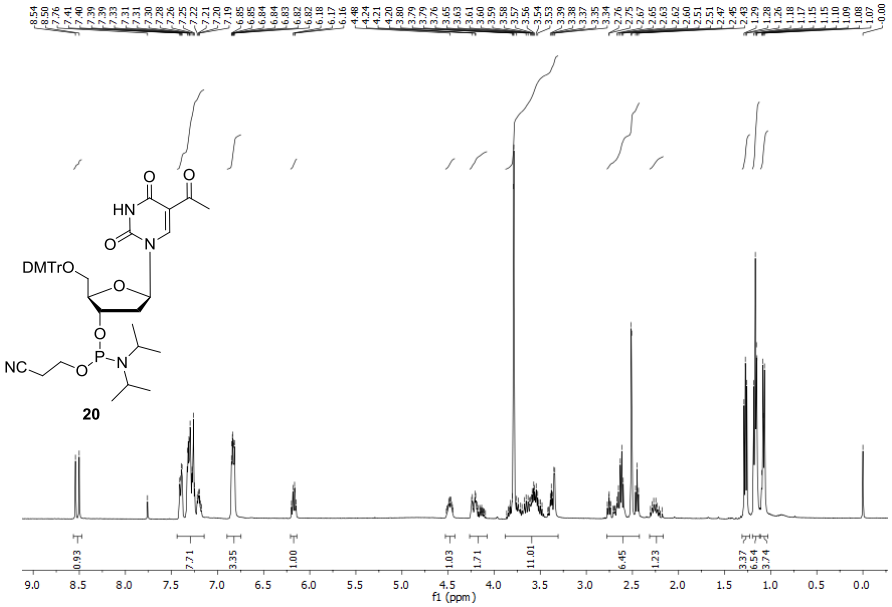

Fig. S35 ^{1}H NMR spectrum of compound **20**.

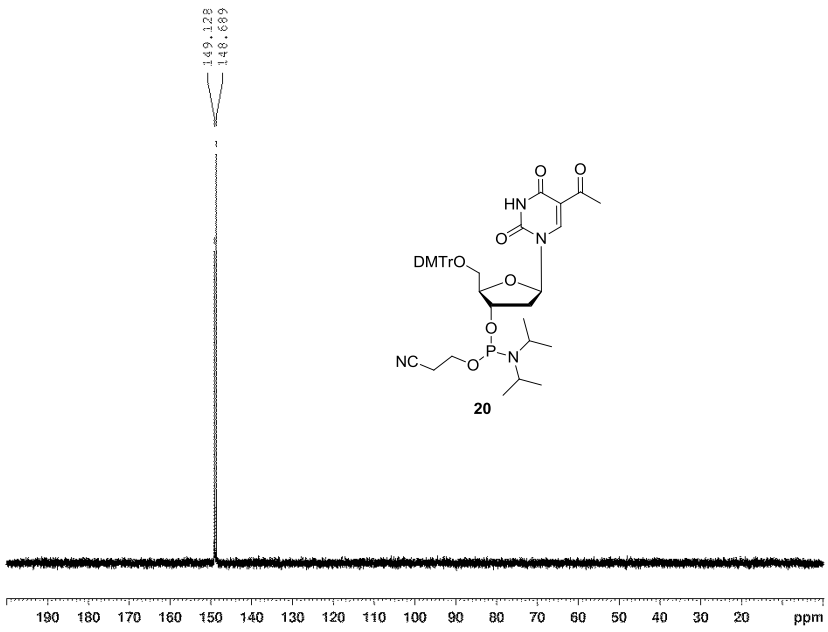

Fig. S36 ^{31}P NMR spectrum of compound **20**.

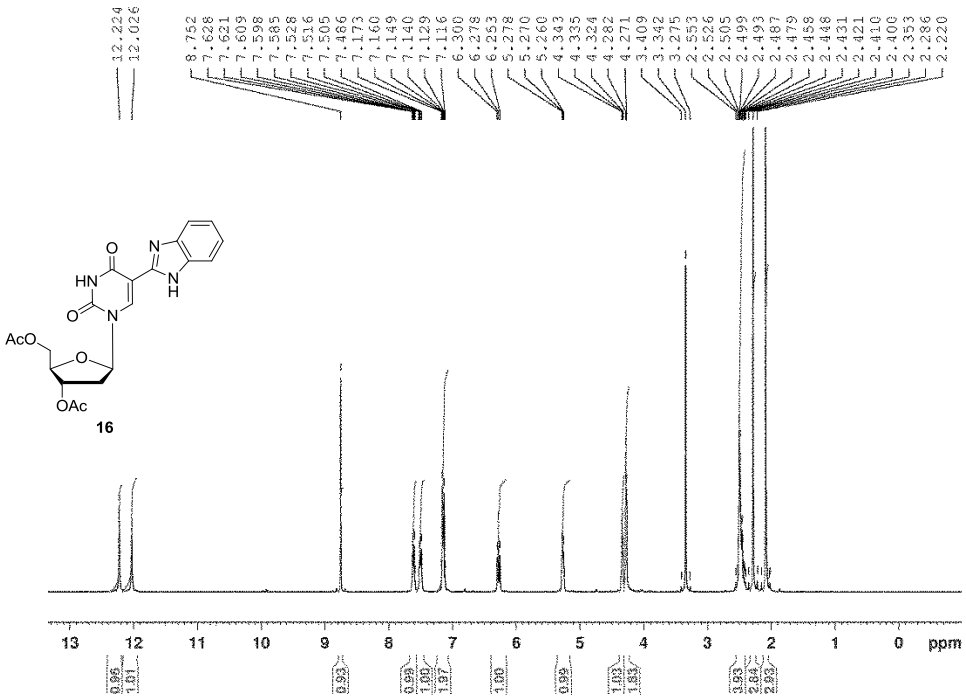

Fig. S37 ^{1}H NMR spectrum of compound **16**.

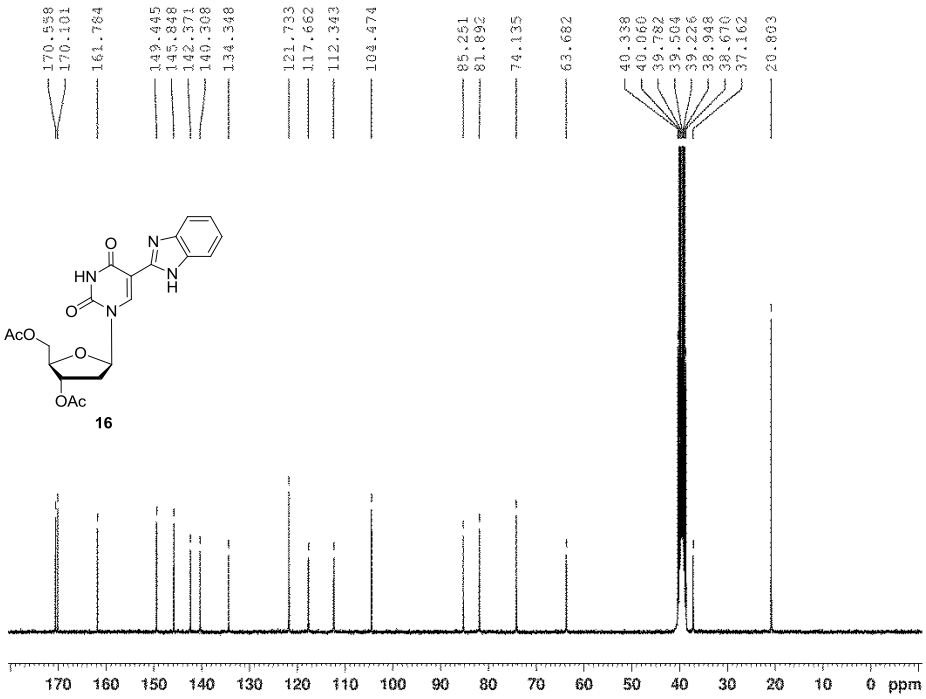

Fig. S38 ^{13}C NMR spectrum of compound **16**.

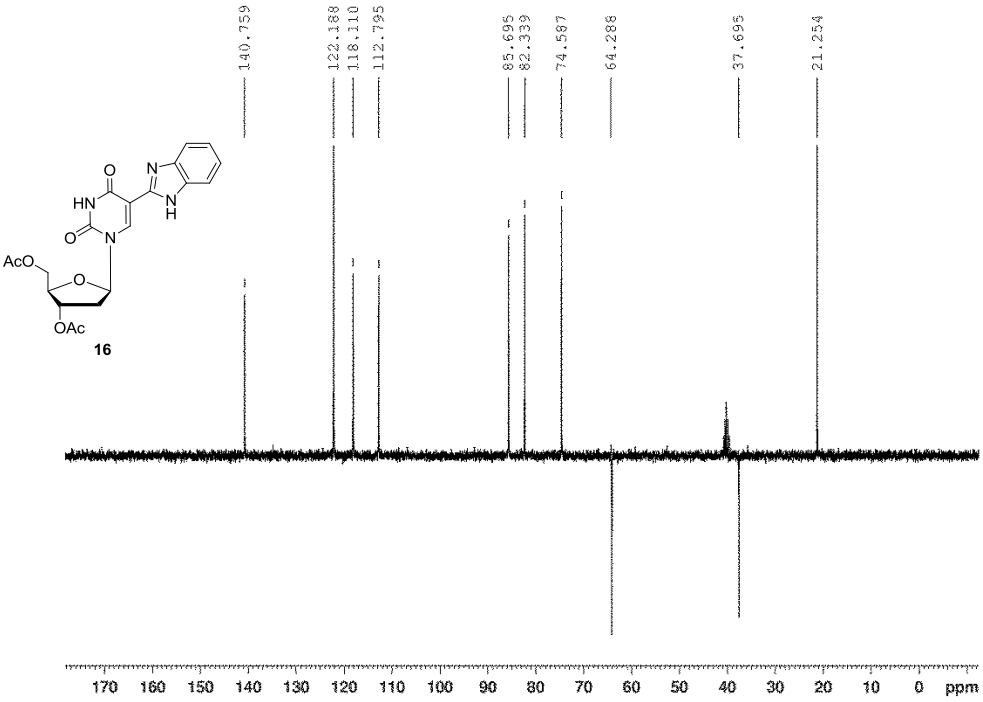

Fig. S39 DEPT-135spectrum of compound **16**.

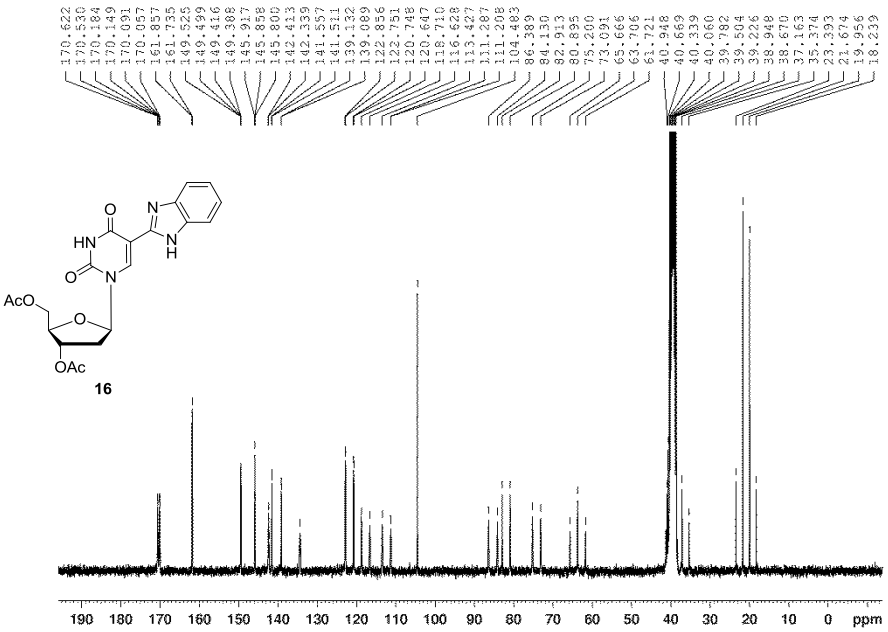

Fig. S40 ^{1}H-^{13}C gated-decoupled spectrum of compound **16**.

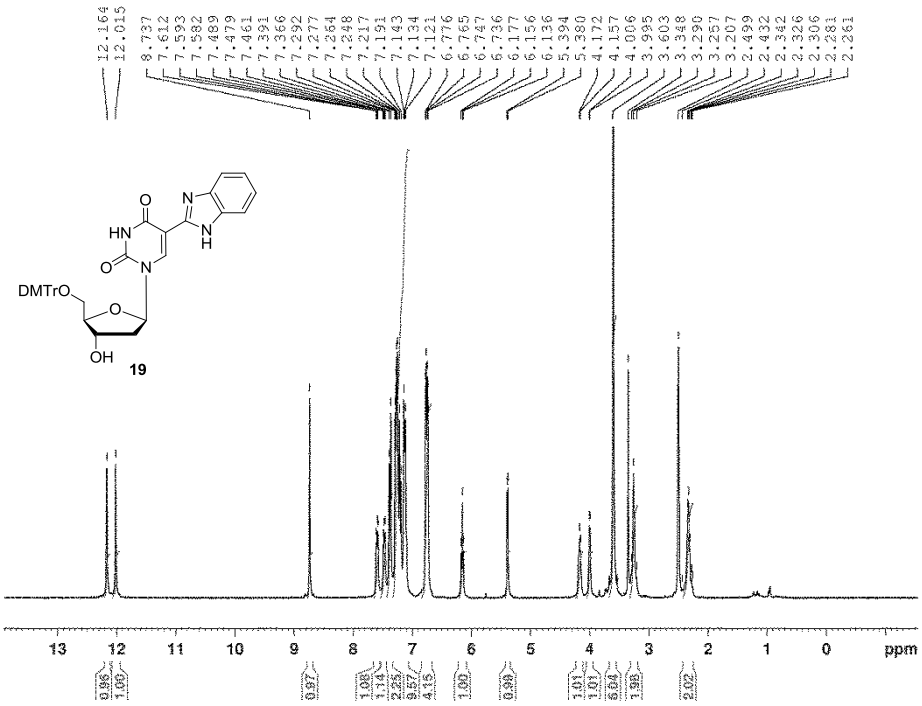

Fig. S41 ^{1}H NMR spectrum of compound **19**.

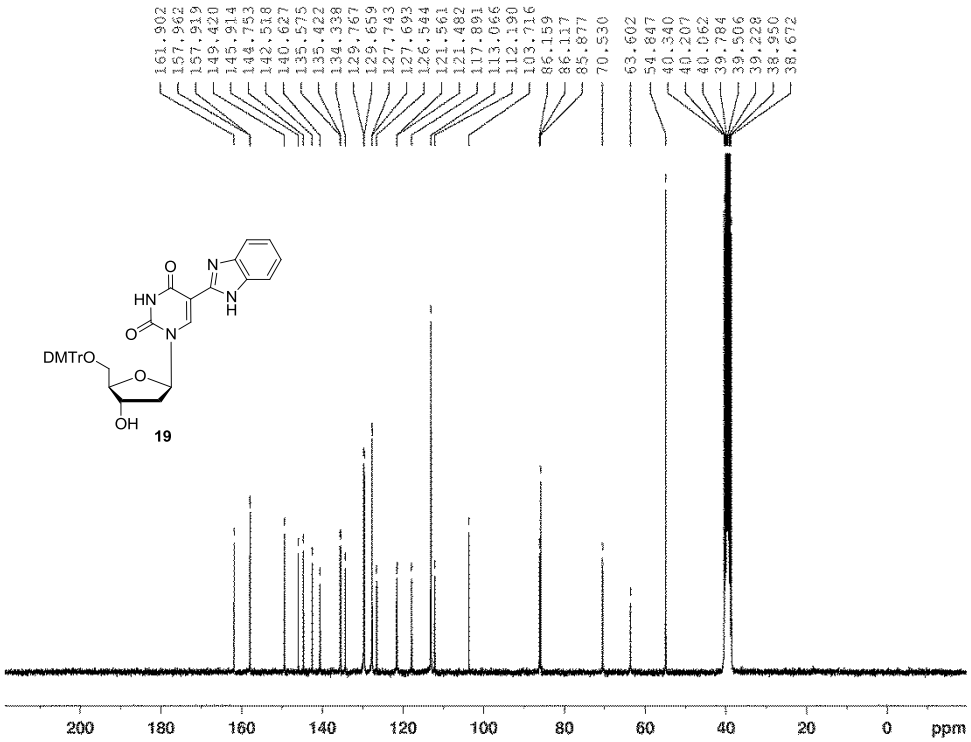

Fig. S42 ^{13}C NMR spectrum of compound **19**.

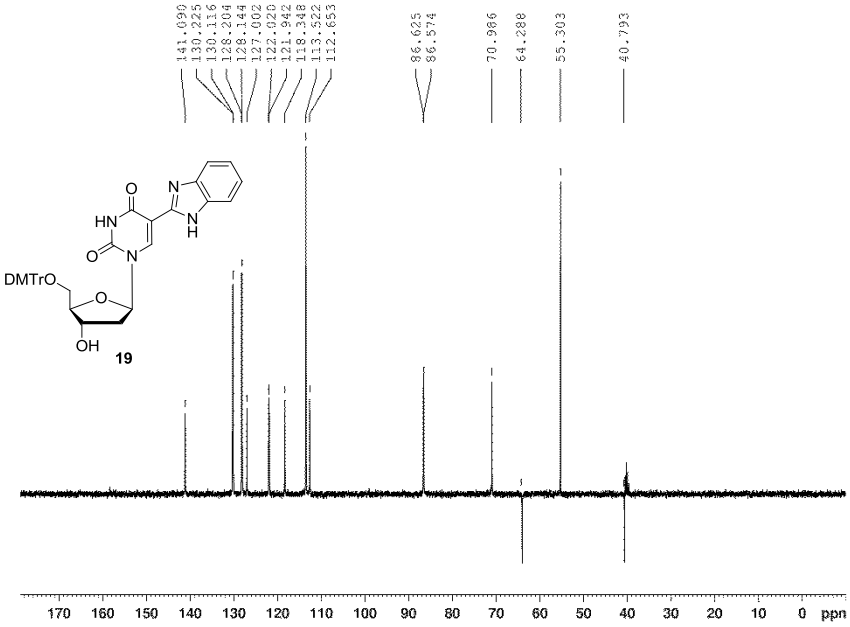

Fig. S43 DEPT-135spectrum of compound **19**.

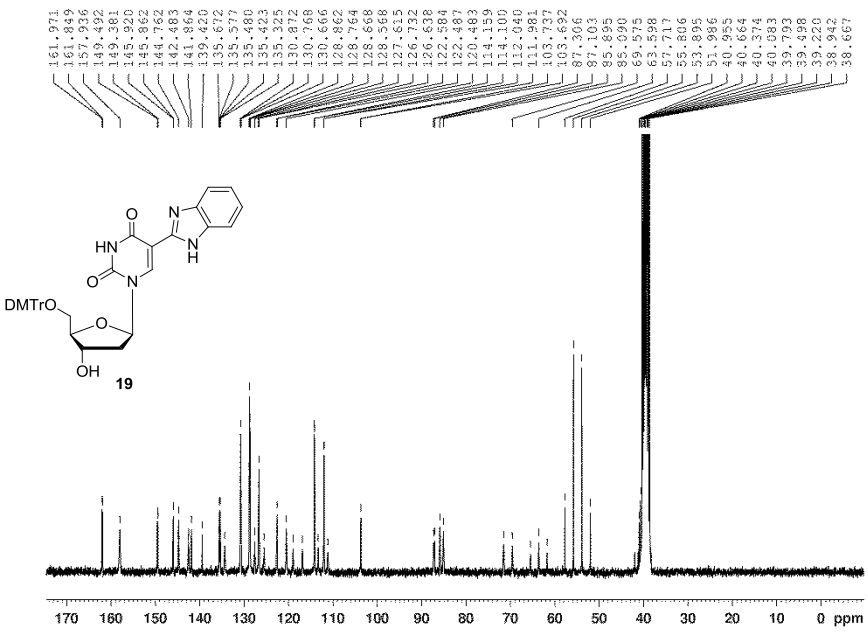

Fig. S44 ^{1}H-^{13}C gated-decoupled spectrum of compound **19**.

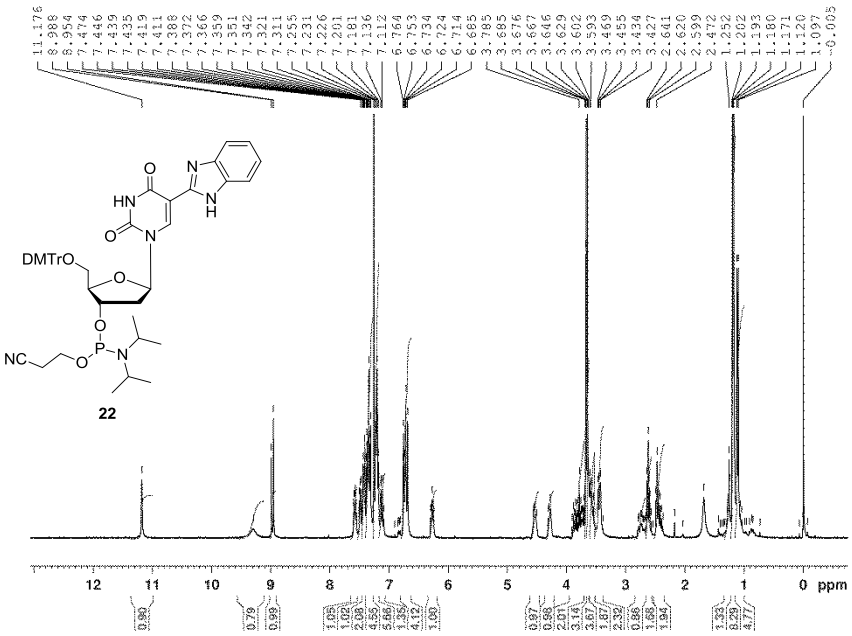

Fig. S45 ^{1}H NMR spectrum of compound **22**.

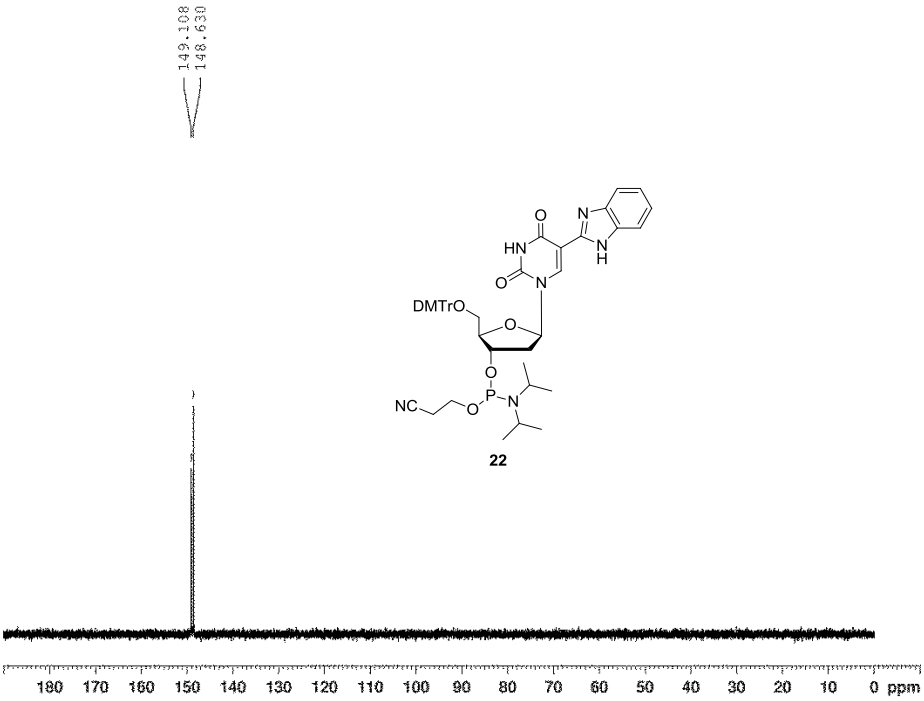

Fig. S46 ^{31}P NMR spectrum of compound **22**.

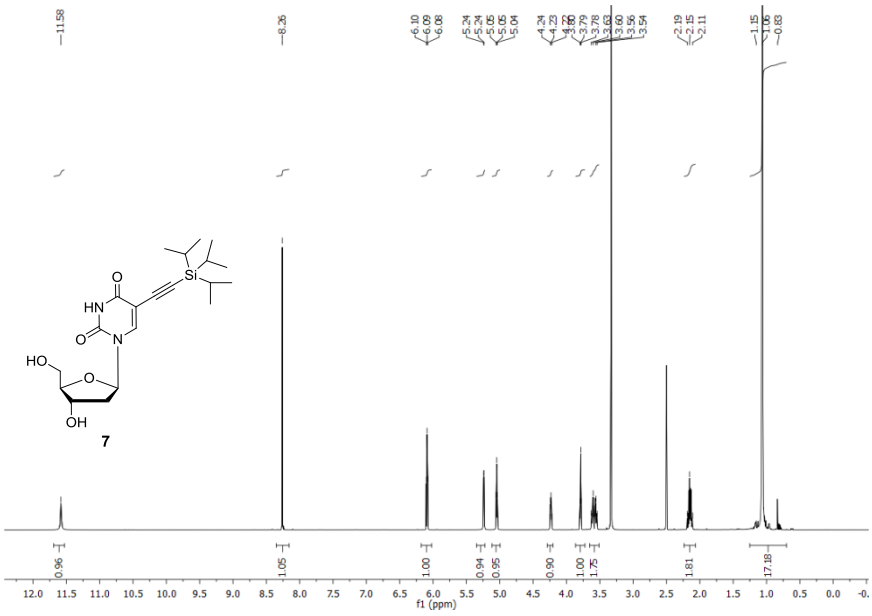

Fig. S47 ^{1}H NMR spectrum of compound **7**.

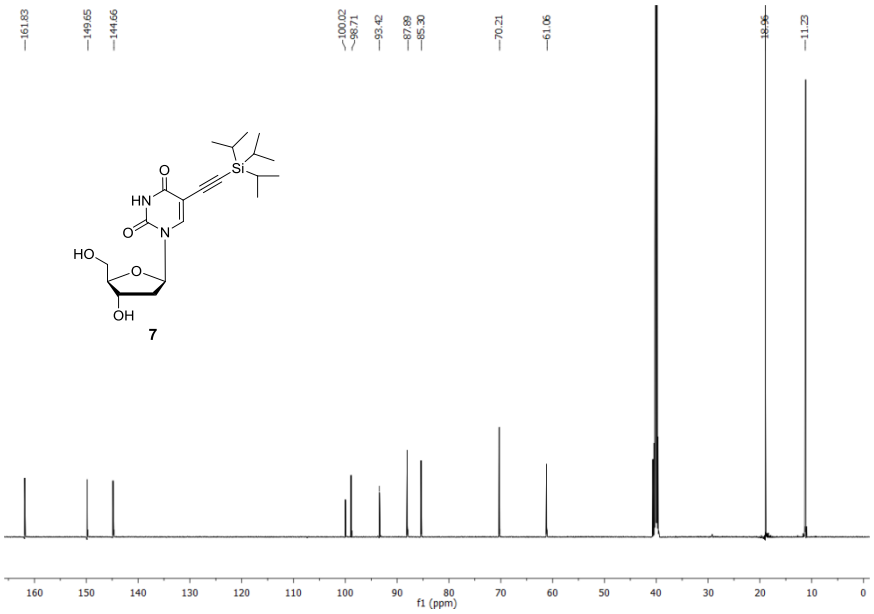

Fig. S48 ^{13}C NMR spectrum of compound **7**.

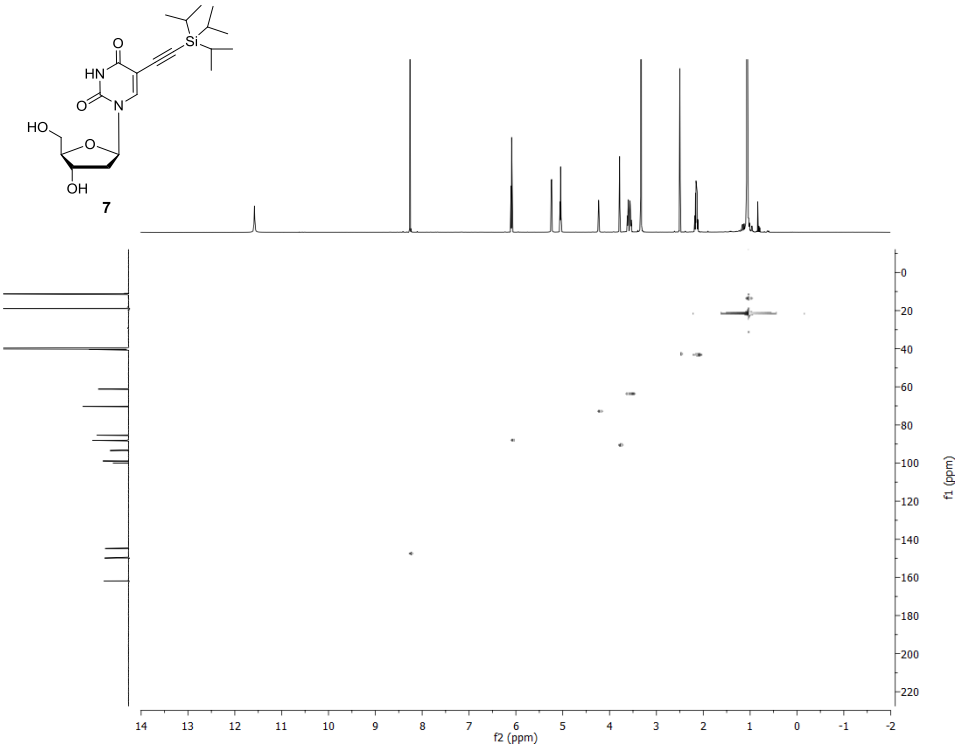

Fig. S49 HSQC spectrum of compound **7**.

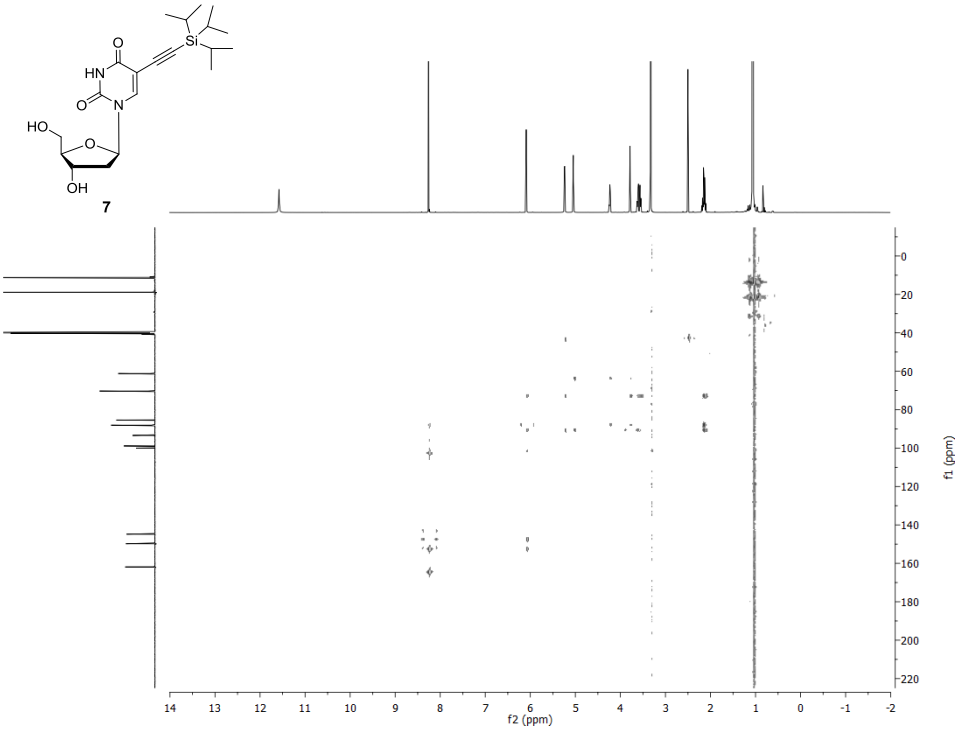

Fig. S50 HMBC spectrum of compound **7**.